Brass Instruments: Linear Stability Analysis and Experiments with an Artificial Mouth

John Cullen, Joël Gilbert, Murray Campbell

Brass Instruments: Linear Stability Analysis and Experiments with an Artificial Mouth

J. S. Cullen
Department of Physics and Astronomy
University of Edinburgh
Mayfield Road
Edinburgh EH9 3JZ
United Kingdom

J. Gilbert
Institut d'Acoustique et de Méchanique de l'Université du Maine
Laboratoire d'Acoustique – UMR CNRS 6613
Avenue Olivier Messaien
72085 Le Mans Cedex 9
France

D. M. Campbell
Department of Physics and Astronomy
University of Edinburgh
Mayfield Road
Edinburgh EH9 3JZ
United Kingdom

June 13, 2000

Abstract

The self-sustained oscillation of a brass wind musical instrument involves a complex aerodynamic coupling between a multimode mechanical vibratory system (the lips of the player) and a multimode acoustical vibratory system (the air column of the instrument). In this paper the behaviour of the coupled system near the threshold of oscillation is investigated using a simplified model in which a single mechanical lip mode is coupled to a single mode of the acoustical resonator. Linear stability analysis is used to study the theoretical variation of threshold blowing pressure and threshold playing frequency as functions of lip and air column parameters. The theoretical results are compared with experimental results obtained from a systematic study of the near threshold behaviour of a trombone sounded by an artificial lip mechanism. Comparability between theory and experiment is ensured by using model parameter values derived from mechanical response measurements on the artificial lips and input impedance measurements on the trombone.

The measured mechanical response curve for the artificial lips exhibits several resonance peaks, each of which can be classified unambiguously as either "inward striking" or "outward striking". For each of these resonance peaks, parameters have been extracted and used in numerical simulation of threshold behaviour as a function of trombone slide extension. However, the experimentally observed threshold frequencies of the coupled system suggest a behaviour which passes smoothly from "inward striking" to "outward striking" character as the trombone slide is extended or the embouchure parameters changed. It seems unlikely that this type of behaviour can be explained using a lip model with only a single degree of freedom.

I INTRODUCTION

I.A General introduction and literature review

Sound production in the brass wind musical instrument family is a result of self-sustained lip oscillation. The mechanical oscillator (the lips of the player), acts as a valve which modulates the air flow through the lips. The destabilization of the mechanical element is the result of a complex aeroelastic coupling between (1) the lips, (2) the air flow entering the instrument due to the static overpressure in the mouth of the musician, and (3) the resonant acoustic field in the instrument itself. The phenomenon thus belongs to the class of flow-induced vibrations, which has been extensively studied both theoretically and experimentally (see, for example, Blevins [1]).

The first global study modelling the behaviour of a 'simplified' player coupled to a brass instrument was proposed by Elliot and Bowsher [2]. Applying the small oscillation hypothesis, they compared experimental measurements obtained using a trombone player with behaviour predicted by their theory. This pioneering work has already been extensively discussed by Campbell and Greated [3]. In the present study Elliot and Bowsher's work is revisited and extended to take into account some flow-induced vibration effects. As pointed out by Elliot and Bowsher, major obstacles in achieving a comprehensive study of the characteristics of brass instrument tone are the number of lip and instrument parameters which can influence the note and the considerable range of values which some of these parameters can take. In order to avoid the difficulty of experimental study on human vibrating lips, an artificial mouth with artificial buzzing lips was developed [4] [5], in which the 'embouchure' is controlled by only a small number of parameters.

The global modelling of brass instruments requires the description of the instrument itself (the acoustic resonator), the mechanical valve (the lips), and the aeroelastic coupling between the valve and the air flow into the instrument. One reasonable model relies on a fairly simple representation of the aeroelastic coupling. Following Elliot and Bowsher, the lips are modelled by one mode of flexural vibration; the description 'one mass motion' or 'one mass model' recalls the single mechanical degree of freedom of this model. The air flow entering the instrument, through the channel between the lips, is assumed to be quasi-stationary, incompressible and frictionless. The coupling to the resonator is obtained by using conservation of volume flow and assuming non-recovery of pressure at the entrance to the mouthpiece due to the creation of a region of turbulent mixing slightly downstream of the flow-separation at the end of the lip channel.

The acoustical behaviour of the mouthpiece and air column of a brass instrument has been extensively studied, with convincing theoretical and experimental results [6] [7] [8] [9]; in comparison, understanding of the behaviour of the buzzing lips is less advanced. Some published observations of human lip oscillations [10] [11] [12] [13] show that the one mass model is not sufficient to describe the lip vibration and a more complex model, analogous to the two mass-model developed for the human vocal folds, must be adopted. However, convincing time-domain simulations based on simple one mass models have been developed [14] [15] [16] [17]. A large portion of the dynamic behaviour of real instruments is already described by these simplified models, which give very realistic sound synthesis. To further improve the synthesis, large amplitude effects such as non-linear behaviour of the lips and lip collisions must be taken into account. In addition, for rasping sounds, nonlinear acoustic propagation in the instrument must be considered [18] [4] [19].

Following the pioneering work of Helmholtz [20] and Bouasse [21], several theoretical and experimental studies have been carried out on the oscillation threshold behaviour of a basic one-mass model coupled with acoustical resonators. Reed woodwind and brass instruments are conventionally separated into two categories: 'inward striking reeds' (the valve closes as the supply pressure increases) and the 'outward striking reeds' (the valve opens as the supply pressure increases). These two categories have very distinct vibrational and acoustic behaviour [22] [23] [24]. From frequency measurements the reed can be classified as 'inward striking' if the threshold playing frequency is lower than both the mechanical and acoustical resonance frequencies or 'outward striking' if the threshold playing frequency is greater than both the mechanical and acoustical resonance frequencies. It has been clearly established that single reed wind instruments exhibit 'inward striking' behaviour [25] [26] [27] [28] [29]. However experimental studies to categorize the lip reed in brass instrument excitation have not produced any definitive conclusions [24] [30] [31] [4] [5].

I.B Aim and contents of this paper

The aim of this study is to contribute to a better understanding of sound regeneration in brass instruments at the threshold of oscillation, and to investigate the flow induced vibrations of the lips. Linear stability analysis of finite dynamical systems provides the main theoretical background. The experimental results were obtained using an artificial mouth. The present paper is divided into three sections. After this brief introduction, the theoretical background is presented in section II. The theoretical discussion makes use of experimental results to be presented in full in section III.

In section II.A the simplified physical model is derived and linearized around the equilibrium position of the lips. These linearized equations are presented in the time domain as two coupled oscillators, equivalent to a finite dynamical system of degree four. The theory of linear stability analysis is briefly reviewed in section II.B; some classic results in the theory of elastic stability are presented, including the flutter effect. Linear stability analysis is then applied to the two coupled oscillator problem; threshold pressure and frequency values predicted by the simple model are presented and discussed in section II.B. That section also investigates the variation in threshold values as a function of various acoustical and mechanical parameters.

The theoretical results presented in section II are not based on new theoretical insight: one mass models of the lips have previously been proposed by several other researchers and, for woodwind instruments, theoretical investigations of threshold values have also been carried out. However the linear stability analysis representation provides an interesting comparison between 'flow induced vibrations' in two aerodynamically coupled mechanical oscillators, and acoustic oscillations in the case of one acoustical oscillator aerodynamically coupled to one mechanical oscillator. Furthermore this paper presents results of simulations which were run using lip parameters and acoustical parameters based entirely on systematic experimental measurements. These measurements are described in section III. Section III.A is devoted to the presentation of the experimental procedures used to measure the acoustical input impedance, the mechanical response of the artificial lips and the oscillation threshold. The experimental results are compared to the theoretical ones in section III.B. Mechanical response measurements are presented for a range of static mouth overpressures from zero (no aeroelastic coupling) to a value slightly below the oscillation threshold. These response measurements were carried out with the artificial lips coupled only to a mouthpiece rim (with the cup removed), and also to a complete mouthpiece. Threshold measurements performed using a trombone coupled to artificial lips are compared to threshold behaviour predicted by the theoretical model. The qualitative features recovered by the simplified one-mass model are extensively discussed and the limits of this approach are considered. The results lead to a discussion of the possibility of including a second mechanical mode in the lip model. Finally the perspectives of this work are discussed in the conclusions.

II THEORY

II.A Brass instruments coupled to lips by air flow: A basic physical model

The basic one mass model

Before studying the linear stability of the lips, the selection of a relatively simple model which provides a reasonable reproduction of the behaviour observed in some limited domain (small oscillations hypothesis) is required. The lips are flexible, continuous structures submitted to aerodynamic forces depending on the pressure field around them (see figure 1a). In this paper the lip motion is approximated by a 'one mass model': each lip is allowed to oscillate with a 1-dimensional motion along an axis defined by the unit vector ϵ, making an angle θ with the vertical x axis (see figure 1b). This angle is determined by the aerodynamic forces acting on the lip. The pair of lips acts as a valve, controlling the air flow into the mouthpiece. It is assumed that the flow control depends only on the vertical component of the motion of the lips, and that the longitudinal component of the lip motion does not generate a significant additional volume flow.

If it is assumed that the two lips are identical, and are placed symmetrically on the mouthpiece, then the dynamics of each lip can be represented by the simple second order oscillator equation

$$\frac{d^2X}{dt^2} + \frac{\omega_L}{Q_L}\frac{dX}{dt} + \omega_L^2 X = \frac{F}{m} \tag{1}$$

where $X(t)$ is the instantaneous distance of each lip from the axis of symmetry at time t. Each lip has natural (angular) frequency ω_L, quality factor Q_L, mass m and is acted on by a force with vertical component F. The dynamics of the entire system (lower lip plus upper lip) can be represented by a single second order oscillator described by the equation

$$\frac{d^2H}{dt^2} + \frac{\omega_L}{Q_L}\frac{dH}{dt} + \omega_L^2 H = \frac{F}{m_L} \tag{2}$$

where $H(t) = 2X(t)$ is the instantaneous distance between the lips at time t and the effective mass of the system is $m_L = m/2$.

The channel between the lips is assumed to have constant width b. The flow through this channel is assumed to be quasi-stationary, frictionless and incompressible; the velocity field in the lip channel is therefore uniform, and its magnitude U_L is determined by the Bernoulli relation

$$P_m = P_L + \frac{1}{2}\rho U_L^2 \tag{3}$$

where P_m is the instantaneous overpressure in the mouth and P_L is the instantaneous overpressure in the lip channel. The velocity in the mouth is not included in equation 3 because the large cross-sectional area of the mouth relative to the area of the lip channel implies that the velocity in the mouth is negligible.

It is assumed that the air flow separates precisely at the exit of the lip channel, forming a thin jet. The velocity of this jet is equal to the velocity in the lip channel; the pressure at the exit of the lip channel is thus equal to the pressure in the lip channel. After the jet has travelled a short distance, it expands rapidly, producing a region of turbulent mixing. Downstream of this region the velocity field can be considered uniform across the entire cross-section of the mouthpiece. Although the velocity decreases as the flow expands, the turbulent dissipation of kinetic energy implies that there will be no pressure recovery across the turbulent region. The pressure in the lip channel, P_L, can therefore be considered to be equal to the pressure at the input of the instrument mouthpiece, P.

If the overpressure, lip separation, velocity, or volume velocity in a region r is A_r then A_r can be written as the sum of the mean (time averaged) value of A_r, $\overline{A}_r$ and the alternating component of A_r, a_r:

$$A_r = \overline{A}_r + a_r. \tag{4}$$

The time averaged overpressure will subsequently be referred to as static pressure.

The alternating pressure in the mouth, p_m, is assumed to be negligible relative to the alternating pressure in the mouthpiece, p, which is equivalent to assuming that the input impedance of the mouth cavity is zero. In this case $P_m \approx \overline{P_m}$. In the current model it is assumed that the static overpressure in the mouthpiece, $\overline{P}$, is negligible relative to the static overpressure in the mouth, $\overline{P_m}$, and therefore $P_L \approx P \approx p$. This assumption has been questioned [32] for the analogous case of a double woodwind reed. In that case the cross-sectional area of the reed opening can exceed that of the neck of the reed, and it seems likely that the pressure drop through the neck would then be of the same order as that across the reed opening. A similar situation could arise in the case of a loudly blown note on a brass instrument, for which the lip opening area could be comparable to the mouthpiece throat. The present study was confined to near-threshold oscillations, for which the lip opening area was considerably smaller than the mouthpiece throat diameter, and the pressure gradient in the throat was neglected.

The pressure field assumed in the model can be summarised as follows: the internal faces of the lips are subjected to a purely static pressure, $\overline{P_m}$, whereas the channel and external faces are subjected to the purely alternating input mouthpiece pressure, p. By applying this simplified pressure field, equation 3 may be expressed in the form

$$\overline{P_m} = p + \frac{1}{2}\rho(\overline{U_L} + u_L)^2 \tag{5}$$

where $\overline{U_L}$ is the mean velocity in the lip channel and u_L is the alternating velocity in the lip channel.

Downstream of the turbulent mixing region the velocity field may be considered uniform across the entire cross-section of the mouthpiece. Conservation of volume flow implies that the volume flow at the entrance to the mouthpiece, V, is equal to the volume flow through the lip channel:

$$\overline{V} + v = b(\overline{H} + h)(\overline{U_L} + u_L) \tag{6}$$

where $\overline{V}$ and $\overline{H}$ are the mean values of V and H, respectively and v and h denote small fluctuations in V and H, respectively, about their mean values.

The total aerodynamic force, F, acting on the lips is often separated into two forces, F_D and F_B, which have opposite effects on the aperture. One of the forces is proportional to the pressure difference between mouth and mouthpiece *i.e.* $F_D/m_L = (\overline{P_m} - p)/\mu_D$, where μ_D is the effective mass of the lips, m_L, divided by the effective area of the internal face of the lips; this force implies an 'outward striking reed behaviour'. The second force is proportional to the pressure in the lip channel, *i.e.* $F_B/m_L = p/\mu_B$ where μ_B is the effective mass in the lip channel divided by the effective area of the channel faces of the lips; this force implies an 'inward striking reed behaviour'. In musical acoustic literature F_B is often named the 'Bernoulli force'. From the above discussion it is clear that the total alternating force per unit mass exerted on the lips is equal to $p/(1/\mu_B - 1/\mu_D)$. Substituting this expression for the right hand side of equation 2, and replacing H with the alternating component of lip separation, h, yields the following expression describing the dynamics of the lip motion:

$$\frac{d^2h}{dt^2} + \frac{\omega_L}{Q_L}\frac{dh}{dt} + \omega_L^2 h = \left(\frac{1}{\mu_B} - \frac{1}{\mu_D}\right) p \tag{7}$$

Equations 5, 6 and 7 form a simple model for the volume flow control by the movement of the lips of the brass player. Many supplementary non-stationary terms neglected here are suggested in the literature, representing, for example, a secondary volume source due to the motion of the lips, the inertial effect of air in the channel and a moving point of flow separation in the neck of the lip channel. The effect of each of these terms can easily be estimated theoretically but it is difficult to choose realistic values for the parameters involved. In the crude model defined above, as there is no a priori evidence that either of the forces F_D or F_B is dominant, the assignment of the lip reed to one of the pressure controlled valve categories initially defined by Helmholtz is not obvious. This problem has been discussed at length in several papers [4] [22] [23] [24] [30] [31] and will be revisited in section III of this paper.

Linearized equations and the two coupled oscillators representation

In order to carry out linear stability analysis equations 5 and 6 must be linearized about the lips' equilibrium position. The linearization is performed by neglecting any terms containing the product of two alternating variables and by neglecting all steady variables which are not multiplied by a single alternating term. This leads to the linearized Bernoulli relation

$$0 = p + \rho\overline{U_L}u_L \tag{8}$$

and the linearized volume flow equation

$$v = b\overline{H}u_L + b\overline{U_L}h. \tag{9}$$

A suitably simplified mathematical model of the acoustic oscillation of the air column is also required. The acoustic input impedance of a brass instrument is defined as $Z(\omega) = p(\omega)/v(\omega)$, where $p(\omega)$ and $v(\omega)$ are the complex pressure and velocity amplitudes, respectively, at the input end of the mouthpiece. A typical input impedance curve for a trombone is shown in figure 8; each of the air column resonances is represented by a well defined peak. In the present study of near-threshold coupled oscillations of the lip-air column system, it is assumed that only a single air column mode participates significantly in a given oscillation regime of the coupled system. If this air column mode has resonance frequency ω_A, peak impedance Z_A, and quality factor Q_A, the input impedance in the frequency region close to ω_A can be represented approximately by the equation

$$Z(\omega) = \frac{Z_A}{1 + 2jQ_A\left(\frac{\omega - \omega_A}{\omega_A}\right)} \tag{10}$$

(see Chang[33], equation 3).

Equation 10 forms the basis of a curve fitting routine used in the present study to extract acoustical parameters from input impedance measurements; the equation will be discussed again in section III. To

incorporate the acoustic resonance into the coupled oscillators formalism we require a time domain representation of equation 10. Making use of the approximation $\omega^2 - \omega_A^2 \approx 2\omega(\omega - \omega_A)$, equation 10 can be rewritten as

$$Z(\omega) = \frac{Z_A}{1 + \frac{jQ_A(\omega^2 - \omega_A^2)}{\omega\omega_A}} \tag{11}$$

which has the equivalent time domain representation

$$\frac{d^2\psi}{dt^2} + \frac{\omega_A}{Q_A}\frac{d\psi}{dt} + \omega_A^2\psi = \left(\frac{Z_A\omega_A}{Q_A}\right)v, \tag{12}$$

where $d\psi/dt = p$.

Equation 7 describes the mechanical oscillator and equation 12 describes one mode of the acoustical oscillator. The v variables in equation 12 can be eliminated by application of the linearized Bernoulli and volume flow equations (8 and 9 respectively). This leads to the following expression for two coupled second order oscillators as a function of h and ψ

$$\frac{d^2}{dt^2}\begin{bmatrix} h \\ \psi \end{bmatrix} + \mathbf{C}\frac{d}{dt}\begin{bmatrix} h \\ \psi \end{bmatrix} + \mathbf{K}\begin{bmatrix} h \\ \psi \end{bmatrix} = 0 \tag{13}$$

where

$$\mathbf{K} = \begin{bmatrix} \omega_L^2 & 0 \\ -\left(\frac{Z_A\omega_A}{Q_A}\right)(b\overline{U_L}) & \omega_A^2 \end{bmatrix} \quad \text{and} \quad \mathbf{C} = \begin{bmatrix} \frac{\omega_L}{Q_L} & \frac{1}{\mu_D} - \frac{1}{\mu_B} \\ 0 & \frac{\omega_A}{Q_A} + \left(\frac{Z_A\omega_A}{Q_A}\right)\left(\frac{b\overline{H}}{\rho\overline{U_L}}\right) \end{bmatrix}. \tag{14}$$

The 2×2 matrices $\mathbf{K}$ and $\mathbf{C}$ are the 'stiffness matrix' and 'damping matrix' respectively.

Equation 13 can easily be arranged into a set of 4 simultaneous first order ordinary differential equations [34] which have matrix representation

$$\frac{d}{dt}\begin{bmatrix} h \\ \psi \\ \frac{dh}{dt} \\ \frac{d\psi}{dt} \end{bmatrix} = \begin{bmatrix} \mathbf{0} & \mathbf{I} \\ -\mathbf{K} & -\mathbf{C} \end{bmatrix}\begin{bmatrix} h \\ \psi \\ \frac{dh}{dt} \\ \frac{d\psi}{dt} \end{bmatrix} \tag{15}$$

where $\mathbf{0}$ is the 2×2 zero matrix and $\mathbf{I}$ is the 2×2 identity matrix.

The interaction of a reed and a resonant air column has been modelled by two coupled simple harmonic oscillators in several previous studies, but only Weinreich [35] and Chang [33] have used a 4×4 matrix representation.

II.B Linear stability analysis, flutter effect and destabilization of the lips

Threshold of instability, flutter effect

Solving problems of vibrations and stability almost inevitably involves solving eigenvalue problems [36]. Many systems with two coupled modes can be modelled by linearizing equations for the system about a 'fixed point' and then writing the linearized equations in the general form

$$\frac{d\mathbf{x}}{dt} = \mathbf{M}\mathbf{x} \tag{16}$$

where $\mathbf{x}$, the vector transpose of $(x_1, x_2, \dot{x_1}, \dot{x_2})$, describes the state of the system and $\mathbf{M}$ is the 4×4 matrix of equation 15. The elements of $\mathbf{K}$ and $\mathbf{C}$ depend on the particular system under consideration.

Each of the four solutions to equation 16 takes the form

$$\mathbf{x} = \mathbf{w}e^{\lambda t} \tag{17}$$

where $\mathbf{w}$ is a four dimensional vector and λ is a complex valued constant. The system is unstable when the real part of λ is greater than zero. Substitution of equation 17 into equation 16 yields the eigenvalue problem

$$(\mathbf{M} - \lambda\mathbf{I})\mathbf{w} = \mathbf{0} \tag{18}$$

for the eigenvalues λ_i and eigenvectors $\mathbf{w}_i$, $i = 1$ to 4. The eigenvalues can be found by solving the equation

$$|\mathbf{M} - \lambda\mathbf{I}| = \mathbf{0}. \tag{19}$$

Figure 2 demonstrates how the eigenvalues can evolve as a function of a control parameter, α. The four eigenvalues are in the form of two complex conjugate pairs but only the eigenvalues with positive imaginary parts are displayed in the figure. Linear stability is preserved provided the real parts of all eigenvalues remain negative but the system becomes unstable when the real part of one of the complex eigenvalue pairs becomes positive. A bifurcation is said to occur when there is a marked qualitative change in the system behaviour [36]. A Hopf bifurcation, which creates periodic oscillations out of equilibriums, occurs when one pair of eigenvalues has purely imaginary parts, $\lambda = \pm j\omega_t$, while the other pair of eigenvalues has negative real parts. Provided the eigenvalue pair does not cross the imaginary axis at the origin, an imaginary axis crossing, induced by a change in α, is accompanied by a Hopf bifurcation, indicating loss of stability and transition to a periodic regime. The threshold (angular) frequency of oscillation is the magnitude of the imaginary axis intercept, ω_t, and the threshold value of the control parameter, α_t, is the value of the control parameter, α at the imaginary axis.

When the fixed point is destabilized and a permanent oscillatory regime is sustained the state variables oscillate with a finite amplitude. The equations describing the system cannot be applied in their linearized form to this situation; information about the permanent oscillatory regimes can only be extracted using the equations in their original nonlinear form. However it is reasonable to assume that the theoretical threshold frequency is approximately equal to the fundamental frequency of a very small amplitude quasi-sinusoidal oscillation. This point will be discussed at the end of section II.

Holmes [34] carried out extensive stability and dynamical studies applied to a fourth order dynamical system representing a coupled two mode model of a pipe conveying fluid. In Holmes' paper, two different generic kinds of stability are defined: flutter and divergence. Flutter is said to occur if the eigenvalues form complex conjugate pairs and at least one complex conjugate pair has positive real parts; divergence occurs if at least one of the eigenvalues is real and positive.

One established example of the flutter effect in flow-induced vibrations is the destabilization of an aircraft wing. Some of the basic conclusions obtained from such aircraft wing studies are briefly reviewed here as they can be applied to the buzzing lips problem. Destabilization of the wings is a result of the flutter effect produced by aerodynamic coupling between two elastic modes; a bending mode and a torsional mode [37]. The flow coupling is modelled by a non-diagonal element in the 'stiffness matrix' which makes the matrix unsymmetric. The introduction of the coupling term causes the natural angular frequencies of the two modes (*i.e.* the magnitudes of the imaginary parts of the eigenvalues) to move towards each other as the air flow speed (the control parameter) increases. This coalescence effect is illustrated in figure 3 for the analogous case of two mechanical modes of the lips coupled by airflow. Rocard [37] pointed out that destabilization does not require the intervention of 'negative resistance' to compensate for structural damping. In fact the destabilization resulting from the coalescence of the mode frequencies can be aided by structural damping, provided the damping remains small: in figure 3 α_t is lower in the damped case than in the undamped case.

The dual mechanical mode approach has already been used to model the vocal folds [38] [39] [40] and, in studies of snoring, has also been applied to the soft palate [41]. Subtle effects in the model can have significant consequences on the flutter behaviour, defining which of the two mechanical modes is destabilized. For example, in Auregan and Depollier's [41] snoring model the first mechanical mode is destabilized if flow induced damping is neglected but the second mechanical mode is destabilized if the flow induced damping resulting from non-stationary flow around the soft palate is included.

Application to the one-mass model

In this section linear stability analysis is applied to the excitation of brass instruments using the simplified model derived in section II.A. In this particular case the control parameter of the flow-induced vibrations is $\overline{P_m}$ and the 'fixed point' is $H(\overline{P_m}) = \overline{H}(\overline{P_m})$, $U_L(\overline{P_m}) = \overline{U_L}(\overline{P_m})$ and $P(\overline{P_m}) = 0$. Recall that, in order to derive equation 15, the Bernoulli and volume flow equations were linearized about the fixed point. It is interesting to note how the 'damping' and 'stiffness' matrices defined in equation 14 describe flow coupling. The inclusion of flow coupling in the model introduces non-zero terms for the bottom left element of the

stiffness matrix, **K**, and the top right element of the damping matrix, **C**. The bottom right element of **C** is also modified by the addition of a second flow induced damping term.

Linear stability analysis was performed on the simplified model by numerically solving the equations of the model (equations 14 and 15) to find the eigenvalues. Each of the simulations presented in section II makes use of realistic parameters obtained from input impedance measurements on a trombone and dynamic and static mechanical response measurements (described in section III.A). To simplify notation the parameter $1/\mu_L = (1/\mu_D - 1/\mu_B)$ is used. For a lip reed with dominant outward behaviour $1/\mu_L > 0$ but for a lip reed with dominant inward behaviour $1/\mu_L < 0$. For each case considered in this section $\overline{H_0} = 0.44\,\mathrm{mm}$, $b = 11\,\mathrm{mm}$ and the control parameter $\overline{P_m}$ was varied between 0 and 100 mbar.

The eigenvalue evolution as a function of $\overline{P_m}$ is displayed in figures 4 and 5 for several different sets of mechanical and acoustical parameters. The two mechanical modes of the systems discussed in Section II.B can be characterised by (angular) resonance frequencies ω_1 and ω_2 and quality factors Q_1 and Q_2. For such systems, when $\alpha = 0$, the eigenvalues are equal to $-\omega_1/(2Q_1) \pm j\omega_1$ and $-\omega_2/(2Q_2) \pm j\omega_2$. However, for the model considered in this section, as $\overline{P_m} \to 0$ (and therefore $\overline{U_m} \to 0$) one eigenvalue pair $\to -\omega_L/(2Q_L) \pm j\omega_L$ while the other two eigenvalues $\to -\infty$ because the c_{22} element $\to \infty$. The system studied here does not exhibit the strong coalescence of eigenfrequencies, due to the 'flutter effect', which was illustrated in section II.B. However figures 4 and 5 do show eigenvalue crossings of the imaginary axis. The eigenvalue crossing, the point at which the equilibrium position becomes linearly unstable, defines what is known as the threshold of stability. The value of the mouth pressure at this point is known as the threshold pressure, P_t; the threshold frequency, f_t, is defined to be the imaginary axis intercept divided by 2π. Figures 4 and 5 indicate that the threshold values are effected by the resonance frequencies and quality factors of the lips and the resonator. They also demonstrate that either of the modes may be destabilized. If the acoustic resonance frequency, f_A, is significantly higher than the lip resonance frequency, f_L, then the acoustical mode, whose eigenvalue increases from -∞, is destabilized; an example of this is shown by the highest curve in figure 5. If f_A is only slightly greater than f_L, or indeed if $f_A \leq f_L$, then it is the the mechanical mode, whose eigenvalue curve starts from one of the points represented by a black circle in figure 5, which is destabilized.

It was noted earlier that numerical evaluation of eigenvalues is not the only method which has been applied to the study of the threshold of stability. Chang [33] carried out a systematic study of reed stability using the Routh test; he produced stability maps in terms of threshold pressure and the ratio of resonance frequencies. Several systematic studies of linear stability have also been carried out using the closed loop transfer analogy [22] [24]; in this method the open loop transfer function condition defines the threshold of stability. Wilson and Beavers [28] investigated the linear stability of a single reed coupled to cylindrical tubes. Their threshold results were presented as a function of one parameter of the tube: its length. A similar presentation is adopted here (in figure 6), where the representative parameter of the resonator, a trombone, is the slide extension.

As there are several acoustical modes and several mechanical modes of the lips (see section III.A), acoustical parameters are distinguished when necessary by the subscript 'An', where n is the acoustic mode number to which the parameter belongs; similarly, lip parameters are given the subscript 'Lm', where m is the mechanical mode number to which the parameter belongs.

The outward reed case of figure 6 was produced using mechanical parameters f_{L1}, Q_{L1} and μ_{L1} deduced from experimental results to be discussed in section III. The threshold behaviour was investigated by repeatedly calculating eigenvalue evolutions with the same mechanical parameters but with different acoustical parameters. For each value of slide extension, x, the acoustical resonance frequencies, quality factors, and magnitudes of input impedance peaks were obtained from a measured impedance curve for the 4th, 5th and 6th acoustical modes. The eigenvalue evolution was then calculated for each mode and used to deduce a total of three pairs of threshold values (P_t, f_t); however only the pair of threshold values with the lowest value of P_t was plotted in figure 6 as that represents the true threshold. This process was repeated for each value of slide extension. The mechanical parameters were then changed to values corresponding to an inward striking reed, and the entire process was repeated.

The $P_t(x)$ curve can be viewed as a prediction of the minimum mouth pressure required by a trombone player to sustain a note with a fixed embouchure characterized by the parameters used in the model and the slide extended to position x. The $f_t(x)$ curve represents the frequency of the note played with slide extension x and mouth pressure P_t.

The inwards striking reed threshold behaviour illustrated in figure 6 was produced using mechanical

parameters f_{L2}, Q_{L2} and μ_{L2} deduced from experimental results to be discussed in section III. In the case of the inward striking reed, f_t is divided into two distinct regimes corresponding, respectively, to the 5th and 6th acoustical modes of the resonator. When the slide extension is at 0 cm, f_t is slightly less than the lip resonance frequency, f_{L2}, and much lower than the resonance frequency of mode 5, f_{A5}, the nearest acoustical mode. As the slide is slowly extended both f_{A5} and f_t decrease, and the difference between f_{A5} and f_t decreases. After the slide has been extended by more than 30 cm f_t jumps up in frequency to slightly below f_{L2}. At this point the oscillation is supported by acoustical mode 6 rather than mode 5. This pattern is repeated for higher modes. Distinct regimes are also apparent from the threshold pressure measurements, although the transitions between regimes are less clear cut than in the case of the frequency curves. The transitions theoretically occur at the intersections of the threshold pressure curves of adjacent regimes. However, P_t has been calculated only at the discrete values of slide extension for which experimentally derived parameters were available, so that the transition points can be deduced from figure 6 only by extrapolation of the pressure curves for adjacent regimes.

In the case of the outward striking reed, f_t is divided into three distinct regimes corresponding, respectively to the 4th, 5th and 6th acoustical modes of the resonator. The threshold behaviour of the outward striking reed is very different to that of the inward striking reed. For a particular regime in the outward striking reed case, as the slide is extended, f_t moves from being slightly above an acoustical resonance frequency (*e.g.* f_{A5}) to being slightly above the lip resonance frequency, f_{L1}. Figure 6 confirms that with the outward striking reed model the playing frequency must always lie above both the lip resonance frequency and the acoustic resonance frequency; with the inward striking reed model the playing frequency must lie below both the lip resonance frequency and the acoustic resonance frequency. In the outward striking reed case the regimes are not so apparent in the threshold pressure curve because the curve does not vary smoothly. This reflects the fact that the curve was calculated using experimentally measured acoustical parameters: as the slide extension is varied the quality factor and shape of the acoustical resonances vary in addition to the acoustic frequency. In section III figure 6 will be compared with playing tests conducted using the artificial mouth.

It is also possible to fix the acoustical parameters and vary the lip parameters. In figure 7 the threshold results are displayed as a function of the frequency and as a function of the lip quality factor. This is a somewhat artificial representation of the lip behaviour as the resonance frequency and quality factor do not vary independently of each other, or the other lip parameters (see section III). However this figure does illustrate several important points. In figure 7 the lip resonance frequency and quality factor vary over a range of values which were observed experimentally using the artificial lips. The other mechanical parameters were held constant in both cases and are typical of the values measured using the artificial lips.

Figure 7a can be viewed as a prediction of the variation of threshold values as a trombone player tightens the embouchure. The note which is produced depends on both the acoustical parameters of the lips and the acoustical parameters of the instrument. With a lip frequency $f_L = 182$ Hz the third acoustical mode of the trombone is excited. In this case f_L lies well above the acoustical resonance frequency, f_{A3}, so it is the mechanical mode which is destabilized, resulting in a threshold frequency, f_t, which is strongly related to f_L. As f_L increases f_t continues to increase. The model predicts that the threshold pressure, P_t, also increases as the oscillation receives less and less support from the acoustical resonance. Eventually the fourth acoustical mode can be excited with a lower value of P_t than would be required for the third mode. Since the resonance frequency of the fourth mode, f_{A4}, lies well above f_L, it is the acoustical mode which is destabilized, so f_t is strongly related to f_{A4}. As f_L is increased further the lip resonance is better able to support the oscillation and so P_t decreases; f_t moves away from f_{A4}, towards f_L, and it is the mechanical mode which is again destabilized. Eventually P_t increases with f_L as the pattern begins to repeat for the higher mode. The $P_t(f_L)$ curve has a local minimum at $f_L = 228$ Hz. The value of f_t corresponding to this value of P_t would probably be perceived by the trombone player to be the frequency of 'the most comfortable note' around mode f_{A4}. The 'outward striking reed' model predicts that it is possible for the player to lip the note above and below the most comfortable note, but not below the acoustical resonance frequency. According to this model, when the player attempts to lip the note below the acoustical resonance frequency a frequency gap is encountered before f_t jumps down to a value well above the lower resonance frequency.

The relative values of the acoustic and lip quality factors determine how strongly the instrument influences the frequency of the note produced. This is illustrated in figure 7b: as Q_L is increased from a low value, f_t continues to lie slightly above f_{A4} until a critical value of Q_L is reached when f_t jumps down to lie slightly

above f_L. The critical value of Q_L required for this transition depends on the acoustical parameters and on the other mechanical parameters. When Q_A is reduced the variation of P_t with f_A is reduced. In this case the 'most comfortable note' is not clearly defined, the instrument does not strongly influence f_t and the player is able to lip the notes over a large frequency range. That partially explains why the serpent is more difficult to play in tune than the trombone since the quality factor of the serpent resonances are generally lower than those of the trombone.

In section III measured threshold values will be compared with the theoretical threshold values predicted using linear stability analysis. The measured threshold pressure will be assumed to be the static mouth pressure required to obtain the permanent periodic regimes with as small an amplitude as is possible; the measured threshold frequency will be assumed to be the fundamental acoustic frequency at that value of mouth pressure. These assumptions are valid only if the characteristic variables of the permanent periodic regime (static mouth pressure and fundamental frequency) tend towards the characteristic variables of the linear threshold (threshold pressure and threshold frequency) as the amplitude of the permanent periodic regime tends to zero. This is true in the case of a direct bifurcation but not in the case of an inverse bifurcation. With an inverse bifurcation the threshold mouth pressure of the permanent periodic regime is actually below the linear threshold (see for example the study by Dalmont et [42], applied to reed instruments). In the present study it is necessary to assume that, in the case of the trombone, each bifurcation is a direct bifurcation. The experiments did not provide any evidence of inverse bifurcations.

III EXPERIMENTAL RESULTS

III.A Experimental Methods

Input impedance measurements

The instrument studied was a King tenor trombone, made around 1960. In order to characterize the acoustical response of the instrument its input impedance amplitude was measured as a function of frequency using a standard technique [43]. Input impedance measurements were made at 1 Hz intervals over the frequency range 50–1000 Hz for each of 22 slide positions at 3 cm intervals corresponding to pitch intervals of around 30 cents. The first acoustical mode was not within the range of measurement, but the parameters of this mode were not required because the first mode was not excited in the threshold measurements. The acoustical parameters are listed in table A of the appendix.

From equation 10, the magnitude of the input impedance near the resonance frequency, ω_A, can be approximated as

$$|Z(\omega)| \approx \frac{Z_A}{\sqrt{1 + 4Q_A^2 \left(\frac{\omega - \omega_A}{\omega_A}\right)^2}} \tag{20}$$

At each slide position the acoustical parameters, Z_A, Q_A and $f_A = \omega_A/2\pi$ were estimated for modes 2 to 6 by numerically fitting equation 20 around local maxima, using an 11 point least squares fit routine. A typical input impedance magnitude curve is displayed in figure 8 along with the least squares fit to the peaks. The acoustical parameters used in the one mass model threshold simulations of section II.B were extracted from such input impedance curves.

Artificial mouth

Both the mechanical response measurements and the threshold response measurements were performed using an artificial mouth. The use of an artificial lip mechanism to replace the human player offers great advantages in long term stability, ease of instrumentation and the ability to make small and reproducible adjustments to the embouchure. The present study used an artificial mouth which is a development of the design introduced by Gilbert and Petiot [44]. The artificial mouth consists of a hermetically sealed box encapsulating a pair of water filled latex rubber lips (figure 9) which are clamped between the instrument mouthpiece and plastic "teeth" (a rectangular piece of perspex with a 2 cm diameter hole in the centre).

Gilbert and Petiot's prototype design was modified to provide means of adjusting the volume of water in the lips while the lips are in situ within the mouth cavity, thus achieving a greater control of the embouchure.

In the prototype design the teeth were in fixed relation with the mouth cavity and the principal embouchure control mechanism adjusted the position of the mouthpiece so as to increase or decrease the pressure of the mouthpiece against the lips. However in the artificial mouth of the present study the mouthpiece is in fixed relation with the mouth cavity and the principal embouchure control mechanism moves the teeth. This new arrangement has the advantage that only the rim of the mouthpiece need be contained within the artificial mouth. Translational displacement of the "teeth" is affected by rotating a screw type control device at the rear of the apparatus. In common with the prototype design, a secondary control mechanism can be used to adjust the tension of the lips, but in this investigation the "teeth" position was the only control parameter varied.

An air pump was employed to maintain the static mouth overpressure, which was measured by a piezoceramic manometer. The alternating pressure in the mouth was measured using a small Knowles microphone positioned immediately behind the teeth. For mechanical response measurements a loudspeaker, mounted on the artificial mouth, was used to generate the alternating pressure in the mouth. Throughout the present series of measurements the artificial mouth was used with a specially constructed mouthpiece with a removable cup section. The mouthpiece, when complete, has a total internal volume of 12.7ml, a Helmholtz resonance of 518 Hz and a quality factor of 7.1. The mouthpiece dimensions are indicated in figure 10.

Mechanical response measurements

The mechanical response of the lips to forcing at frequency ω is defined as

$$C(\omega) = \frac{h(\omega)}{p_m(\omega)}. \tag{21}$$

Recall that $h(\omega)$ is the complex amplitude of the alternating component of the distance between the lips and $p_m(\omega)$ is the complex amplitude of the alternating component of pressure in the mouth. For mechanical response measurements this pressure was produced by the loudspeaker. The lip parameters ω_L, Q_L and μ_L can all be deduced from mechanical response measurements [4].

The apparatus used for measuring the mechanical response is shown in figure 11. A laser beam was expanded, passed through the lip aperture in the artificial mouth and brought to focus on a light sensitive diode. Obviously it would be impossible to use this experimental arrangement with a human player. The position of the upstream lens was adjusted until the beam diameter was slightly larger than the mean distance between the lip, $\overline{H}$, but smaller than the width of the lip channel, b. With this arrangement the diode voltage was considered to be directly proportional to the distance between the lips, H. Neutral density filters were inserted in the path of the laser beam to reduce the beam intensity, avoiding saturation of the diode. To optimize the response measurements it was important to select carefully the attenuation of the neutral density filters. The diode was calibrated by replacing the lips of the artificial mouth with a variable width single slit and measuring the diode voltage as a function of slit width. A graph of diode voltage, S_d, versus slit width was plotted; the best fit straight line through the data points had gradient $m = 10.8 \pm 0.2$V/mm and S_d axis intercept $S_{d0} = 0.46 \pm 0.06$V. The lip separation, H, can therefore be deduced from the diode voltage, S_d using the relation

$$S_d = mH + S_{d0} \tag{22}$$

However in the measurement of mechanical response it is the alternating component of lips displacement, h, which is of interest. Inspection of equation 22 reveals

$$h = \frac{s_d}{m} \tag{23}$$

where s_d is the alternating component of the diode signal.

The P.C. supplied a sine wave signal to the loudspeaker, enabling mechanical response measurements to be made at 5 Hz intervals over the frequency range 100–600 Hz. Each sinusoidal frequency burst was of 1s duration so a complete sweep was obtained in 101 s. The signals from the diode and the Knowles microphone were passed through identical 60–900 Hz bandpass filters before they were sampled with a 4096 Hz sample frequency. Identical filters were used to ensure the filtering process did not introduce an additional phase difference between the two signals. Further filtering was applied in the digital signal processing: for each of the 101 frequency bursts, both signals were windowed and Fast Fourier Transformed and the amplitude

and phase of the Fourier series components at the excitation frequency, ω, were extracted. The phase angle of the mechanical response, $\angle C(\omega)$, was calculated using the relation $\angle C(\omega) = \angle S_d(\omega) - \angle S_m(\omega)$, where $\angle S_d(\omega)$ and $\angle S_m(\omega)$ are the phase angles of the diode and microphone signals, respectively. The amplitude of the mechanical response, $|C(\omega)|$, was calculated using the relation $|C(\omega)| = k|S_d(\omega)|/(m|S_m(\omega)|)$, where $|S_d(\omega)|$ and $|S_m(\omega)|$ are the amplitudes of the diode and microphone signals respectively, m is the gradient of the diode calibration curve and k is the Knowles microphone calibration factor over the frequency range considered. A typical mechanical response curve of the lips is shown in figure 12.

For mechanical response measurements the dynamics of the lip motion, near a resonance frequency, ω_L, are described by equation 24 (recall $1/\mu_L = (1/\mu_D - 1/\mu_B)$).

$$\frac{d^2h}{dt^2} + \frac{\omega_L}{Q_L}\frac{dh}{dt} + \omega_L^2 h = \frac{p_m}{\mu_L} \tag{24}$$

From this equation the following expression for the frequency response of the lips can easily be derived

$$C(\omega) = \frac{h(\omega)}{p_m(\omega)} = \frac{-j\frac{Q_L}{\omega\omega_L}\frac{1}{\mu_L}}{1 + \frac{j2Q_L(\omega^2-\omega_L^2)}{\omega\omega_L}} \tag{25}$$

A mechanical mode can be categorized as 'inward striking' or 'outward striking' purely from $\angle C(\omega_L)$, the phase of the mechanical response evaluated at the resonance frequency. From equation 25 it is clear that $\angle C(\omega_L) = -\pi/2$ for dominant outward striking reed behaviour ($\mu_L > 0$) but $\angle C(\omega_L) = \pi/2$ for dominant inward striking reed behaviour ($\mu_L < 0$). Elliot and Bowsher [2] and Adachi and Sato [16] used different definitions of mechanical response; in their models the phase angle of the mechanical response is $+\pi/2$ for an outward striking reed and $-\pi/2$ for an inward striking reed.

From equation 25 it is clear that near the resonance frequency, ω_L, the magnitude of the mechanical response can be approximated as

$$|C(\omega)| = \frac{\frac{Q_L}{\omega_L^2}\frac{1}{|\mu_L|}}{\sqrt{1 + 4Q_L^2\left(\frac{\omega-\omega_L}{\omega_L}\right)^2}}, \tag{26}$$

provided the substitutions $\omega^2 - \omega_L^2 \approx 2\omega(\omega - \omega_L)$ and $\omega\omega_L \approx \omega_L^2$ are made. For each mechanical response curve measured the lip parameters $|\mu_L|$, Q_L and $f_L = \omega_L/2\pi$ were estimated for each mode by numerically fitting equation 26 around local maxima, using a 5 point least squares fit routine. This approach to estimating the lip parameters is similar to that applied to the extraction of acoustic parameters from input impedance magnitude curves. It was not possible to produce an accurate fit to strongly unsymmetrical or indistinct peaks.

The mechanical response curve in figure 12 shows 3 distinct modes with resonance frequencies $f_{L1} = 223\,\text{Hz}$, $f_{L2} = 260\,\text{Hz}$ and $f_{L3} = 393\,\text{Hz}$. From the phase curve it is clear that the f_{L1} mode has dominant outward reed behaviour whereas modes f_{L2} and f_{L3} have dominant inward reed behaviour. There is no evidence of a strong response near the Helmholtz resonance frequency of the mouthpiece (517 Hz).

Mechanical response measurements were carried out for a variety of embouchures with a large range of sub-threshold static mouth pressure values. All response measurements were performed without the trombone but with the mouthpiece, or only the mouthpiece rim, fitted to the artificial lips. Experiments were carried out to investigate whether changing the Helmholtz resonance of the mouth had any effect on the mechanical response of the lips.

Threshold measurements

The apparatus used to produce the threshold measurements is displayed in figure 13. To determine the threshold value for a particular embouchure setting and particular position of the trombone slide, the mouth pressure was slowly increased until a stable sound was obtained.

To remove any inconsistencies in the determination of the threshold, a miniature Knowles microphone was positioned just inside the bell of the trombone; the experimental threshold pressure was defined as the mouth pressure required to produce a microphone signal with a predefined (small) amplitude. The threshold frequency was measured by a digital frequency meter connected to the microphone.

Two different situations were investigated: (1) variation of threshold values as a function of slide extension, with fixed embouchure, and (2) variation of threshold values as a function of embouchure, with slide in a fixed position. Situation (1) corresponds to continuous variation of acoustical parameters with fixed mechanical parameters while situation (2) corresponds to continuous variation of mechanical parameters with fixed acoustical parameters. The embouchure was varied by rotating the teeth control in steps of 1/8 rotations and was always moved from tightest position to slackest position.

III.B Comparison with theoretical results obtained from the linear stability analysis

Static mechanical response measurements

The results of a brief investigation into the response of the lips to a purely static mouth pressure are presented before the dynamic mechanical response measurements (described in section III.A) are discussed. Measurements with purely static pressure were used to determine the lip parameters b and $\overline{H_0}$, and to test the assumptions regarding the pressure field surrounding the lips, which were made in section II.A.

By setting all of the alternating components to zero in the Bernoulli and volume flow relations (equations 5 and 6 respectively) and combining these equations to eliminate U_L, the following relationship between static mouth pressure and volume flow was obtained.

$$\sqrt{\overline{P_m}} = \left(\sqrt{\frac{\rho}{2}}\right) \frac{\overline{V}}{b\overline{H}} \tag{27}$$

A simple flow meter with a rotary float was inserted in the air supply pipe, between the valve and the artificial mouth. With a fixed embouchure, the volume flow was increased from $6\,\mathrm{L\,min^{-1}}$ in intervals of $2\,\mathrm{L\,min^{-1}}$; for each value of volume flow the pressure in the mouth was read off from the manometer. Measurements made with 3 different embouchures are displayed in figure 14. In each case the plot of $\sqrt{\overline{P_m}}$ versus V is a straight line graph, indicating that the variation of $\overline{H}$ with $\overline{V}$ is much less significant than the variation of $\overline{P_m}$ with $\overline{V}$, *i.e.* $\overline{H} \approx \overline{H_0}$, where $\overline{H_0}$ is the distance between the lips when the alternating and static mouth pressure is zero. Using equation 27, estimates of the lip opening area, $b\overline{H_0}$, were made from the gradients of the straight line graphs of figure 14.

The electronic filters were removed from the experimental set-up, allowing the (constant) distance between the lips to be deduced from the D.C. diode signal. Initial measurements, with $P_m = 0$, were carried out to determine H_0 for each of the three embouchures, 'tight', 'medium', and 'slack', considered above.

This experimental arrangement was also used to study the variation of $\overline{H}$ with $\overline{P_m}$ (figure 15). Notice that when the rest of the mouthpiece is added to the rim section the measured values of $\overline{H}$ are systematically reduced by about 5%. The discrepancy is due to a slight misalignment of the laser beam which resulted in the mouthpiece backbore blocking a small percentage of the beam and therefore slightly reducing the intensity of light detected by the diode. Measurements were carried out with $\overline{P_m} \geq 0$ (air flow through lips out of mouth) and with $\overline{P_m} \leq 0$ (air flow through lips into mouth).

When $\overline{P_m} > 0$ there is little variation of $\overline{H}$ with $\overline{P_m}$, confirming the earlier observation that $\overline{H} \approx \overline{H_0}$. Following the discussion of the pressure field surrounding the lips (section II.A), with $\overline{P_m} > 0$, it is expected that the static overpressure in the lip channel, $\overline{P_L}$ should be equal to zero because the static overpressure in the mouthpiece, $\overline{P}$, is zero and there is no recovery of pressure. In this case there is no Bernoulli force, $\overline{H} - \overline{H_0} = \overline{P_m}/(\omega_L^2 \mu_D)$ and so a plot of $\overline{H}$ versus $|\overline{P_m}|$ should give a straight line graph with positive gradient. With $\overline{P_m} < 0$ it is expected that $\overline{P_L} = \overline{P_m}$ and so the F_B and F_D forces both act to close the lips: $\overline{H} - \overline{H_0} = \overline{P_m}(1/(\omega_L^2 \mu_D) + 1/(\omega_L^2 \mu_B))$. Since $\overline{P_m} < 0$ a plot of $\overline{H}$ versus $|\overline{P_m}|$ should give a straight line graph with negative gradient and the magnitude of the gradient should be greater than in the $\overline{P_m} > 0$ case.

In figure 15, as expected, the gradient is clearly negative in the $\overline{P_m} < 0$ case. However, for the $\overline{P_m} > 0$ case the gradient is actually slightly negative indicating there must be a significant Bernoulli force. Hirschberg [45] has shown that the Bernoulli force may indeed act under these conditions: the inclusion of viscous effects in the flow can lead to retarded flow separation within a diverging lip channel. As a result the velocity of the jet is less than the velocity at the neck of the lip channel, and a pressure gradient, which acts to close the lips, is created in the lip channel.

Figure 16 shows that, in the $\overline{P_m} \leq 0$ case, the gradient of the $\overline{H}$ versus $\overline{|P_m|}$ curves increase as the embouchure is slackened. This demonstrates that the total 'static stiffness' (which is proportional to the parallel combination of $\omega_L^2 \mu_D$ and $\omega_L^2 \mu_B$) decreases as the embouchure is slackened. In the $\overline{P_m} \geq 0$ case the two forces acting on the lips oppose each other; the measurements were insufficiently accurate to permit measurments of 'static stiffness' in that situation.

Dynamic response measurements for 3 different embouchures, as a function of mouth pressure

A 'typical' mechanical response curve was presented in figure 12. There were three distinct modes: the first mode, with resonance frequency $f_{L1} = 223\,\text{Hz}$, displayed 'outward striking' behaviour but the higher modes, with resonance frequencies $f_{L2} = 260\,\text{Hz}$ and $f_{L3} = 393\,\text{Hz}$, both demonstrated 'inward striking' behaviour. In figure 17 mechanical response curves, measured with $\overline{P_m} = 0$, are displayed for the three embouchures considered in Section III.B; each of the mechanical response measurements represented in figure 17 was made with the mouthpiece cup removed, leaving only the rim. The resonance frequencies increase as the embouchure is tightened. However in each case there is a strong resonance with outward character around 180–230 Hz and one with inward character around 330–400 Hz. The 180–230 Hz and 330–400 Hz resonances correspond, respectively, to the f_{L1} and f_{L3} resonances of the 'typical' case. In figure 17, from the magnitude curve alone there is little evidence of a resonance corresponding to f_{L2}. However for the 'medium' and 'tight' embouchures the phase curve crosses the $\pi/2$ line around 250-270Hz, providing some evidence of f_{L2} resonances. There are also weaker resonances with 'outward' character around 150 Hz.

The above measurements were repeated with the entire mouthpiece in place (figure 18). Figures 17 and 18 are of similar shape but the scale of the magnitude curves are very different; the measurements with the entire mouthpiece systematically underestimate the magnitude of the mechanical response due to the slight misalignment of the laser beam, described in connection with the static measurements in Section III.B. Blocking some of the light near the edge of the beam does not greatly effect the D.C. component of the diode signal but can greatly reduce the amplitude of the A.C. component, since $\overline{H} \gg h$ for mechanical response measurements.

Figure 19 demonstrates how the mechanical response evolves as the static mouth pressure is increased from zero to a value just below the threshold of oscillation. As $\overline{P_m}$ increases the aerodynamic coupling increases with the result that the quality factor of one or more mechanical modes increases, tending towards infinity. Notice that the 250–270 Hz resonance with 'inward' character, equivalent to f_{L2} of the 'typical' curve, can only be clearly distinguished when $\overline{P_m} \neq 0$. The real and imaginary components of the eigenvalues are related to the quality factor and natural frequencies of the modes: $Re[\lambda]/2\pi = -f_L/(2Q_L)$ and $Im[\lambda]/2\pi = f_L$. It is interesting to plot the measured evolution of $(-f_L/(2Q_L),\ f_L)$ as a function of $\overline{P_m}$ (figure 20) as this representation is analogous to the theoretical complex plane eigenvalue evolution (for example figure 4). With this representation, as $\overline{P_m}$ increases the horizontal component moves towards the vertical axis.

It is interesting to compare the mechanical response measurements presented here with the preliminary measurements of Gilbert et al [4], who used an artificial mouth of similar design but fitted with only one lip. In that study a mechanical mode with 'outward' behaviour and natural resonance frequency of approximately 200 Hz was measured, but no other modes were detected above 100 Hz. The 200 Hz mode corresponds to the mode labelled f_{L1} in the present study. Gilbert et al pointed out that they were able to measure modes with 'outward' behaviour but not modes with 'inward' behaviour (such as the f_{L2} and f_{L3} modes in the present study), since the displacement of the lip was measured using a laser vibrometer which was sensitive only to longitudinal movement of the lip.

Figure 21 represents the mechanical response of the three embouchures with $\overline{P_m}$ selected to be slightly below the threshold of oscillation in each case. There is no evidence of destabilization of the f_{L1} mode, with outward character. Both modes f_{L2} and f_{L3} appear to be heading towards destabilization. The mouth pressure was then further increased until one of the modes was destabilized, resulting in self sustained oscillation. With the 'tight' embouchure the threshold playing frequency was very close to the f_{L3} resonance, indicating that it was the f_{L3} resonance which was destabilized; with the 'medium' and 'slack' embouchures the f_{L2} resonance appeared to be destabilized. As the embouchure is varied from the 'slack' position to the 'tight' position there is a bifurcation of the periodic regime associated with f_{L2} to the periodic regime associated with f_{L3}. This unexpected behaviour supports the mouthpiece playing frequency measurements of Gilbert et al [4] (figure 5); they observed two discrete oscillation regimes, one at 250 Hz and one at 400 Hz.

The lips of the artificial mouth did not buzz when the mouthpiece cup was removed, leaving only the rim. However, to investigate whether there was any evidence of a destabilizing effect even with the cup removed, mechanical response measurements were performed for increasing values of $\overline{P_m}$. In figure 22 the quality factor of the second mode (250Hz) increases with $\overline{P_m}$, indicating the mode is heading towards destabilization. There is no significant increase in the quality factor of the first mode, indicating the first mode is substantially stable. With the acoustical coupling to the mouthpiece now removed, the third mode also appears stable. However its resonance frequency does increase as $\overline{P_m}$ increases, which suggests the mode could still be sensitive to airflow coupling. It is not clear if the destabilizing effect on the second mode is due to aerodynamic coupling to another mechanical mode or to aerodynamic coupling between the lips and the acoustical resonator formed by the mouth cavity [46]. It is worth noting that any possibility of flow control by the mouthpiece throat is certainly absent in the measurements with rim only.

Mouth cavity effect

Experiments were carried out to determine the influence of the mouth cavity on the mechanical response of the artificial lips. The mechanical response of the lips was measured with the mouth cavity in its usual state. The mouth cavity was then partially filled with solid material, reducing the volume of the cavity by approximately 30%, and the mechanical response of the lips was measured a second time. Finally, the solid material was removed and the mechanical response was measured again, with the original mouth cavity volume. Throughout the measurements the embouchure was held constant. Measurements were carried out firstly with the mouthpiece cup removed and $\overline{P_m} = 0$ (figure 23), and secondly with the entire mouthpiece fitted and $\overline{P_m}$ just below the threshold of oscillation (figure 24). There is no clear evidence that the mechanical response of the lips is significantly affected by the modification to the mouth cavity.

In the literature, the ability of brass players to 'buzz' their lips without a mouthpiece is sometimes explained by the mouth cavity effect: destabilization of the lips occurs due to aerodynamic coupling between the lips and the acoustical resonator formed by the mouth cavity [46]. The results of the present experiment do not support this hypothesis. However, even if the mouth cavity is not crucial for destabilization of the lips it could still have a significant effect on other aspects of brass instrument acoustics. For example, in the case of the didgeridoo, the player varies the mouth cavity to alter the timbre of the sound.

Mechanical response evolution with embouchure

The mechanical response measurements presented above were performed using only three different embouchures. The contour map (figure 25) indicates how the mechanical response evolves with embouchure as the embouchure varies over twenty different positions. The contour shading indicates the decibel mechanical response ($10\log_{10}[|C(\omega)|/C_0]$) of a particular embouchure (indicated on vertical axis) to forcing at frequency f (indicated on horizontal axis). The lighter the shading of the map, the stronger the mechanical response. The same reference level, C_0, was used for each embouchure; C_0 was selected to be the maximum value of mechanical response magnitude. The measurements were performed with the mouthpiece cup removed and with $\overline{P_m} = 0$.

The contour map was produced using measurements performed several weeks after the measurements presented in previous sections, but examination of the resonance frequencies suggest that the early measurements with embouchures 'slack', 'medium' and 'tight' have similar mechanical response to contour map measurements with the embouchure positioned at, respectively, 3, 7 and 11 1/8 rotations from the slackest position. The new measurements have similar form to the measurements presented in previous sections but the magnitude of the new response measurements is systematically lower. The range of parameter values extracted from the contour map response measurements are presented in table 2 and a complete list of the parameter values are displayed in table B of the appendix. These parameters were used to select the range of f_L and Q_L for figure 7 and to select parameter values for additional threshold simulation measurements presented in section section III.C.

The 180–220 Hz mode (previously labeled f_{L1}) and the 300–400 Hz mode (f_{L3}) can be clearly distinguished on the contour map, but as $\overline{P_m} = 0$ there is no clear evidence of the intermediate f_{L2} mode. For slacker embouchures an additional mode at around 160 Hz is also apparent. As the embouchure is tightened f_{L2} and f_{L3} increase in frequency.

Lip parameter values

The measuremnets of mechanical response of the artificial lips presented in sections III.B–III.B allow an estimation of the lip parameters required to run the one mass oscillation threshold simulations developed in section II. The output from the simulations will be presented in section III.C.

The measured lip parameters for the embouchures labeled 'slack', 'medium' and 'tight' are presented in table 1. Estimates for the ranges of the lip parameters are displayed in table 2, alongside values used by other authors. The 'present study' estimates of b and $\overline{H_0}$ are extrapolations of the b and $\overline{H_0}$ values listed in table 1. The ranges of f_{L1}, Q_{L1} and $1/\mu_{L1}$ in table 2 were estimated from the values in table 1 and from the additional measurements used to generate the contour map (figure 25). The ranges of f_{L2}, Q_{L2}, and $1/\mu_{L2}$, in table 2, were estimated from the values of table 1 and from mechanical response measurements performed with identical embouchure positions to the contour map measurements but with $\overline{P_m}$ =3 mbar. In table 2 only the parameter values of modes f_{L1} ('outward striking') and f_{L2} ('inward striking') are displayed because, for the acoustic resonators considered in section III.C, initial runs of the simulation indicated that mode f_{L3} could only be destabilized with unrealistically high values of $\overline{P_m}$.

The parameter estimates in the 'present study', Elliot and Bowsher [2] and Saneyoshi et al [24] were extracted from measurements with either a trombone or a euphonium mouthpiece. All of the 'present study' parameters were obtained by direct measurement, using the artificial lip reed mechanism. Not all of the parameters used by Saneyoshi et al or Elliot and Bowsher were measured directly: although some parameters were deduced from measurements with human players others were estimated using inverse calculations which assume the correctness of the one mass model.

The other authors considered a larger range of lip resonance frequencies than in the present study; the ranges of frequency dependent parameters quoted in table 2 are in all cases those appropriate to the range of f_{L1} and f_{L2} observed in the present study. Inevitably the various authors have used different notation. Table 3 indicates the relationship between the parameters used in the various studies; individual papers should be consulted for explanation of the notation.

From table 2 it is obvious that there is a considerable variety in the range of parameter values selected by the various authors. In particular the lip quality factor used by Elliot and Bowsher appears exceptionally low compared to the Saneyoshi et al and 'present study' estimates. Elliot and Bowsher based their estimate of lip quality factor not on measurements of the lips but on measurements by Ishizaka et al. [47] of the mechanical response of human neck and cheek flesh. There appears to be no experimental justification for the choice of lip quality factor by Saneyoshi et al. The ratios of effective area to effective mass ($1/\mu_{L1}$ and $1/\mu_{L2}$) measured in the present study are slightly lower than the values adopted by Saneyoshi et al., and much lower than the values used by Elliot and Bowsher.

III.C Threshold behaviour of buzzing lips coupled to a trombone

In this section simulated threshold behaviour is compared with the threshold behaviour measured using a trombone coupled to the artificial lips.

Fixed embouchure, variable slide length

Immediately before conducting each set of threshold measurements, the mechanical response of each embouchure was measured with $\overline{P_m} = 0$ and the parameters f_{L1}, Q_{L1} and $1/\mu_{L1}$ were extracted. The parameters f_{L2}, Q_{L2} and $1/\mu_{L2}$ were extracted from the $\overline{P_m} = 3$ mbar measurements. The b and $\overline{H_0}$ values were estimated from the values in table 1 and from extrapolations of these values. The acoustic parameters extracted from input impedance measurements are listed in table A of the appendix.

Figure 26 demonstrates how the threshold values vary as the trombone slide is extended. The simulated behaviour was presented earlier in this paper (as figure 6), and was discussed in some detail. It has been reproduced as figure 26b to allow direct comparison with the equivalent threshold measurements (figure 26a). The measured range of threshold pressure is similar to the range predicted by the inward striking model. The outward striking model predicts much higher threshold pressure values, but they are still within a range which a human player could easily produce. Both measurements and simulation demonstrate distinct regimes corresponding to the 4th, 5th and 6th modes of the acoustical resonator. The regimes are apparent in the variation of threshold frequency and, to a lesser extent, in the variation of threshold pressure. The

experimental measurements of slide position at the transitions between regimes do not coincide with the regime transition slide positions predicted by either the inward striking or outward striking models. Figure 27 examines how the threshold behaviour is effected by a change of embouchure and demonstrates that the inward striking model does capture the qualitative threshold behaviour: both measurements and simulation show that tightening the embouchure increases threshold pressures and frequencies and shortens the slide extension required for the transition from acoustical mode 5 to mode 6.

With a fixed embouchure, it is found that for some slide positions the threshold frequency is above the measured acoustic resonance frequency, for others the situation is reversed. This agrees with earlier playing frequency measurements on cup mouthpiece instruments which indicate the playing frequency may be either above or below the instrument resonance frequency, depending on playing conditions [31] [48] [4]. Simple one mass models cannot explain this behaviour: with such models the threshold frequency is always below the acoustic resonance frequency (inward striking reed) or always above the acoustic resonance frequency (outward striking reed). A two mass model coupling the mode with outward striking characteristics, f_{L1}, to the mode with inward striking characteristics, f_{L2}, would allow the threshold frequency to lie above or below the acoustical resonance frequency, depending on the acoustic resonator conditions. Future work will include the implementation of threshold value simulations based on the two-mass model. Two-mass models have already been considered by Adachi and Sato [16]. Several additional terms, which have also been considered in previous studies, such as non-stationary flow terms [2] [24] or terms to model the effect of the mouth cavity and vocal tract [2], could also be added to the current model. Additional terms can easily be added to the one-mass model; the difficulty is in selecting realistic values for the additional parameters.

Fixed slide length, variable embouchure

With the trombone slide fixed in the unextended position, threshold measurements were performed as a function of embouchure position. The embouchure was set in turn to each of the twenty positions used to produce the contour plot (figure 25); the embouchure was varied from tightest position to slackest position. The simulations were run using the lip parameters listed in table B of the appendix.

In figure 7 the threshold values vary only as a function of lip resonance frequency, f_L. Figure 28b is similar to figure 7a, but offers a more realistic representation since the parameters f_L, Q_L and $1/\mu_L$, extracted from experimental measurements, all vary with embouchure. In figure 7a the position of the local minimum in the threshold pressure curve clearly defines the 'most comfortable note'. The experimental measurements (figure 28a) indicate that the threshold pressure varies slowly with embouchure so the 'most comfortable note' is not so well defined. The outward striking reed model of figure 28b also shows a wide range of embouchures (0–9) when the threshold pressure does not vary significantly with pressure. However the inward striking model suggests that, around f_{L1}, the 'most comfortable note' is produced with an embouchure 2/8 rotations from slackest position and around f_{A4} the 'most comfortable note' will be produced with an embouchure slightly tighter than the tightest embouchure of figure 28b.

The experimental measurements indicate that, for the tightest embouchures, the threshold frequency lies slightly above f_{L2}, the resonance frequency of the lip mode with inward striking character. This effect cannot be explained by the simple one mass model.

IV CONCLUSIONS

In this study a simplified model of the self–sustained oscillations of brass instruments was developed, using a one–mass model of the lips. Following Elliot and Bowsher [2], the lips and the acoustical resonator were each represented as simple harmonic oscillators. After making several assumptions about the pressure field around the lips, the air flow through the lips, which couples the two oscillators, was modelled. The basic equations describing the system were linearized about the equilibrium position of the lips and then arranged into four simultaneous first order differential equations.

The theory of linear stability analysis was discussed in a general context, then applied to the specific case of the one-mass lip reed model. The complex plane eigenvalue evolution was briefly studied, but particular emphasis was placed on investigating the variation of threshold values with changes in acoustical and mechanical parameters.

The measurements presented in section III demonstrate that the mechanical response of the artificial lip mechanism is complicated and involves three strong mechanical modes, one mode with outward character and two modes with inward character. Mechanical response measurements as a function of static mouth pressure suggest that the mouthpiece 'buzz' can result from destabilization of the two modes with inward character (modes 2 and 3). However oscillation threshold measurements demonstrate that the mode with outward character (mode 1) is also important when the lips are coupled to a trombone. There is no experimental evidence that the acoustical resonance of the mouth cavity has a significant influence on the stability of the lips.

The static and dynamic mechanical response measurements presented in this paper provide the first 'direct' measurement of lip parameters. The lip quality factors measured in this study are higher than the values which other authors have used in their simulations, while the measured ratio of effective area to effective mass is consistently lower than the values previously adopted.

The measured threshold values were compared with the theoretical threshold values predicted using linear stability analysis applied to the one-mass model. The experimental threshold pressure was considered to be the static mouth pressure required to sustain a permanent periodic regime with a predetermined small amplitude. This is a reasonable assumption provided the bifurcation is a direct bifurcation. There was found to be good qualitative agreement between the measured and simulated oscillation threshold behaviour. The discrepancies between experiment and simulation are no greater than the discrepancies encountered by Wilson and Beavers in their investigation of single reed instruments [28]. However in most instances the simulations presented in this paper overestimate the threshold pressure and fail to accurately predict the slide/embouchure positions at the transition between different regimes. More importantly, the measurements showed that, with a fixed embouchure, for some slide positions the threshold frequency is above the measured acoustic resonance frequency; for other slide positions the situation is reversed. The one-mass model cannot explain this behaviour. The existence of two different mouthpiece buzzing regimes is also inconsistent with the one-mass model [4].

Initial simulations coupling a two-mass lip model to a one-mass representation of the acoustical resonator have failed to demonstrate the strong coalescence of the mechanical modes which has been observed in studies of the soft palate [41]. However the mechanical response measurements presented in this paper suggest the possibility of coupling between the 1st and 2nd mechanical modes when the static mouth pressure is just below the threshold of oscillation. Future work will include the implementation of threshold simulations based on the two-mass model, using the lip parameters presented in the current study.

Acknowledgments

The authors would like to express gratitude to Jean–Francois Petiot, Arnold Myers, Maarten van Walstijn and Narumon Emarat for helpful suggestions and general assistance throughout the course of this work. The financial support of EPSRC, CNRS and the Royal Society is gratefully acknowledged.

Bibliography

[1] R.D. Blevins. *Flow-induced Vibration*. Robert E. Krieger Publishing Company, 1986.

[2] S.J. Elliot and J.M. Bowsher. Regeneration in brass wind instruments. *J. Sound Vib.*, 83:181–217, 1982.

[3] D.M. Campbell and C. Greated. *The Musician's Guide to Acoustics*. Dent, 1987.

[4] J. Gilbert, S. Ponthus, and J.F. Petiot. Artificial buzzing lips and brass instruments: Experimental results. *J. Acoust. Soc. Am.*, 104:1627–1632, 1998.

[5] J.S. Cullen, J. Gilbert, D.M. Campbell, and C.A. Greated. Acoustical measurements in resonators driven by an artificial mouth, oscillation threshold behaviour. In *Proc. ISMA 1998*, pages 141–146, Leavenworth, WA, USA, June 1998.

[6] J. Backus. Input impedance curves for the brass instruments. *J. Acoust. Soc. Am.*, 60:470–480, 1976.

[7] R.L. Pratt, S.J. Elliott, and J.M. Bowsher. The measurement of the acoustic impedance of brass instruments. *Acustica*, 38:236–246, 1977.

[8] S.J. Elliot, J.M. Bowsher, and P. Watkinson. Input and transfer response of brass wind instruments. *J. Acoust. Soc. Am.*, 72:1747–1760, 1982.

[9] R. Caussé, J. Kergomard, and X. Lurton. Input impedance of brass musical instruments– comparison between experiment and numerical models. *J. Acoust. Soc. Am.*, 75:241–254, 1984.

[10] D.W. Martin. Lip vibrations in a cornet mouthpiece. *J. Acoust. Soc. Am.*, 13:305–308, 1942.

[11] H. Bailliet, X. Pelorson, B. Richardson, and T. Lallouache. Lip vibration and pressure recordings during french horn playing. In *Proc. ISMA 1995*, Dourdan, France, 1995.

[12] D.C. Copley and W.J. Strong. A stroboscopic study of lip vibrations in a trombone. *J. Acoust. Soc. Am.*, 99:1219–1226, 1996.

[13] D. Ayers. New perspectives on the brass instruments. In *Proc. ISMA 1998*, pages 1959–1960, Leavenworth, WA, USA, June 1998.

[14] W.J. Strong and J.D. Dudley. Simulation of a player–trumpet system. In *Proc. SMAC'93*, pages 520–524, 1993.

[15] P. Dietz and N. Amir. Synthesis of trumpet tones by physical modeling. In *Proc. ISMA 1995*, Dourdan, France, 1995.

[16] S. Adachi and M. Sato. Trumpet sound simulation using a two-dimensional lip vibration model. *J. Acoust. Soc. Am.*, 99:1200–1209, 1996.

[17] X. Rodet and C. Vergez. Physical models of trumpet-like instruments: Detailed behaviour and model improvements. In *Proc. ICMC 1996*, Hong-Kong, 1996.

[18] A. Hirschberg, J. Gilbert, R. Msallam, and A.P.J Wijnands. Shock waves in trombones. *J. Acoust. Soc. Am.*, 99:1754–1758, 1996.

[19] R. Msallam, S. Dequidt, S. Tassart, and R. Caussé. Physical model of the trombone including non-linear propagation effects. In *Proc. ISMA 1997 in Proc. Institute of Acoustics*, volume 19, pages 419–424, Edinburgh, UK, 1997.

[20] H.J.F. Helmholtz. *On the Sensation of Tones (*1877). Translated by A.J.Ellis, reprinted by Dover, 1954.

[21] H. Bouasse. *Instruments á Vent.* Reprinted (in French) by Delagrave, 1986.

[22] N.H. Fletcher. Excitation mechanisms in woodwind and brass instruments. *Acustica*, 43:63–72, 1979.

[23] N.H. Fletcher. Autonomous vibration of simple pressure-controled valves in gas flows. *J. Acoust. Soc. Am.*, 93:2172–2180, 1993.

[24] J. Saneyoshi, H. Teramura, and S. Yoshikawa. Woodwind and brasswind instruments. *Acustica*, 62:194–210, 1987.

[25] J. Backus. Small-vibration theory of the clarinet. *J. Acoust. Soc. Am.*, 35:305–313, 1963.

[26] C.J. Nederveen. *Acoustical Aspects of Woodwind Instruments.* Knuf, 1969.

[27] W.E. Worman. *Self-sustained nonlinear oscillations of medium amplitude in clarinet-like systems.* PhD thesis, Case Western Reserve University, 1971.

[28] T.A. Wilson and G.S. Beavers. Operating modes of the clarinet. *J. Acoust. Soc. Am.*, 56:653–658, 1974.

[29] J.P. Dalmont, B. Gazengel, J. Gilbert, and J. Kergomard. Some aspects of tuning and clean intonation in read instruments. *Applied Acoustics*, 46:19–60, 1995.

[30] S. Yoshikawa. Acoustical behavior of brass player's lips. *J. Acoust. Soc. Am.*, 97:1929–1939, 1995.

[31] F.C. Chen and G. Weinreich. Nature of the lip reed. *J. Acoust. Soc. Am.*, 99:1227–1223, 1996.

[32] A. P. J. Wijnands and A. Hirschberg. Effect of a pipe neck downstream of a double reed. In *Proc. ISMA 1995*, pages 148–151, Dourdan, France, 1995.

[33] Y.M. Chang. Reed stability. *Journal of Fluids and Structures*, 8:771–783, 1994.

[34] P.J. Holmes. Bifurcations to divergence in flow induced oscillations: A finite dimensional analysis. *J. Sound Vib.*, 53:471–503, 1977.

[35] G. Weinreich. Remarks on the reed-air column system as coupled oscillators. In *Proc. 123rd ASA*, page 2374, April 1992.

[36] J.J. Thomsen. *Vibrations and Stability, Order and Chaos.* McGraw-Hill, 1997.

[37] Y. Rocard. *General Dynamics of Vibrations.* Translated and reprinted by Crosby Lockwood & Son Ltd., 1960.

[38] K. Ishizaka and J. Flanagan. Synthesis of voiced sounds from a two-mass model of the vocal cords. *Bell Syst. Tech. J.*, 51:1233–1268, 1972.

[39] X. Pelorson, A. Hirschberg, R.R. Van Hassel, A.P.J. Wijnands, and Y. Auregan. Theoretical and experimental study of quasi-steady flow separation within the glottis during phonation: Application to a modified two-mass model. *J. Acoust. Soc. Am.*, 96:3416–3431, 1994.

[40] N.J.C. Lous, G.C.J. Hofmans, R.N.J. Veldhuis, and A. Hirschberg. A symetrical two-mass vocal-fold model coupled to vocal tract and trachea, with application to prosthesis design. *Acustica*, 84:1135–1150, 1999.

[41] Y. Aurégan and C. Depollier. Snoring : Linear stability analysis and in-vitro experiments. *J. Sound Vib.*, 188:39–54, 1995.

[42] J.P. Dalmont, J. Gilbert, and J. Kergomard. Reed instruments, from small to large amplitude periodic oscillations and the helmholtz motion analogy. Accepted for publication in Acustica, 2000.

[43] Campbell D.M. Input impedance measurements on historic brass instruments. *Proc. Institute of Acoustics*, 9:111–118, 1987.

[44] J. Gilbert and J.F. Petiot. Brass instruments, some theoretical and experimental results. In *Proc. ISMA 1997 in Proc. Institute of Acoustics*, volume 19, pages 391–400, Edinburgh, UK, 1997.

[45] R.J. Hirschberg, J. Kergomard, and G. Weinreich, editors. *Mechanics of Musical Instruments*, pages 311–317. Springer–Verlag, 1995.

[46] N.H. Fletcher and T.D. Rossing. *The Physics of Musical Instruments*, pages 355–359 & 391–392. Springer-Verlag, first edition, 1991.

[47] K. Ishizaka, J. C. French, and J. Flanagan. Direct determination of vocal tract impedance. *I.E.E.E. Transactions on Acoustic Speech and Signal Processing*, ASSP-23:370–373, 1975.

[48] J.S. Cullen, D. Batty, D.M. Campbell, and D.B. Sharp. Acoustical investigation of the cornetto (abstract). In *Proc. Forum Acusticum 1996*, page 183, Antwerp, Belgium, April 1996.

[49] V.V. Bolotin. *Nonconservative Problems of the Theory of Elastic Stability*. Pergamon Press, 1963.

Figures

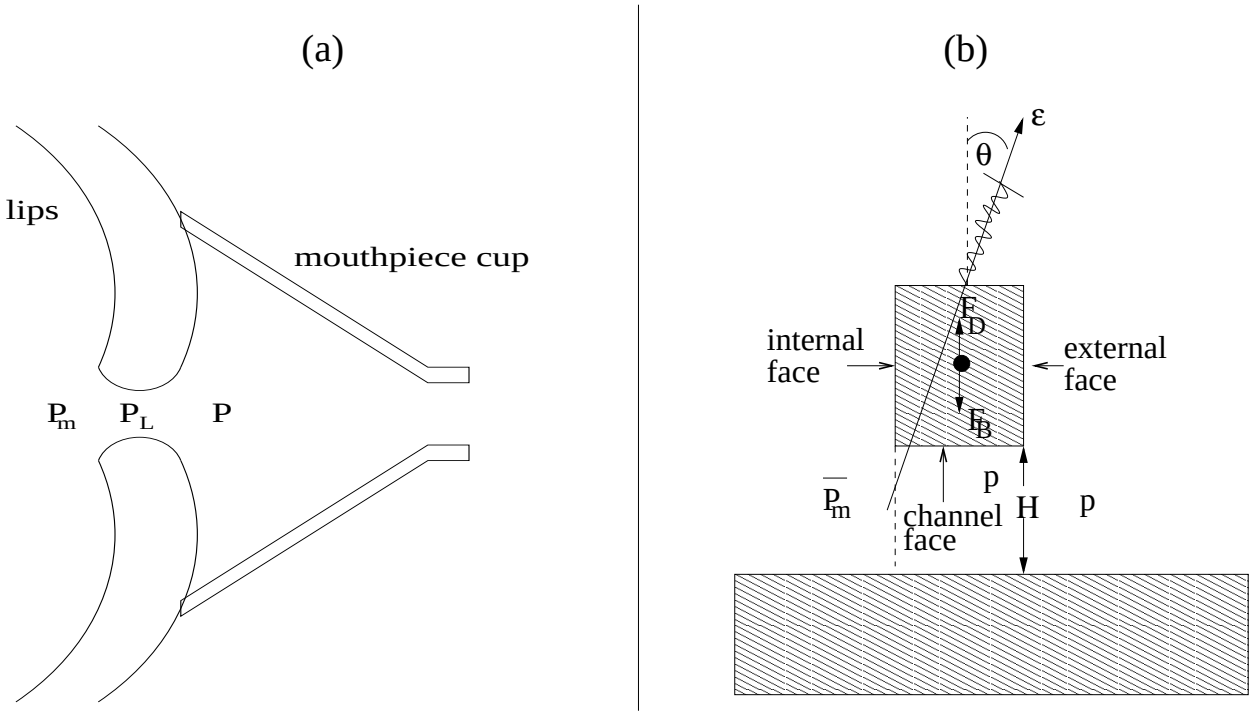

Figure 1: (a) Two continuous flexible lips. (b) One-mass model of lip vibration.

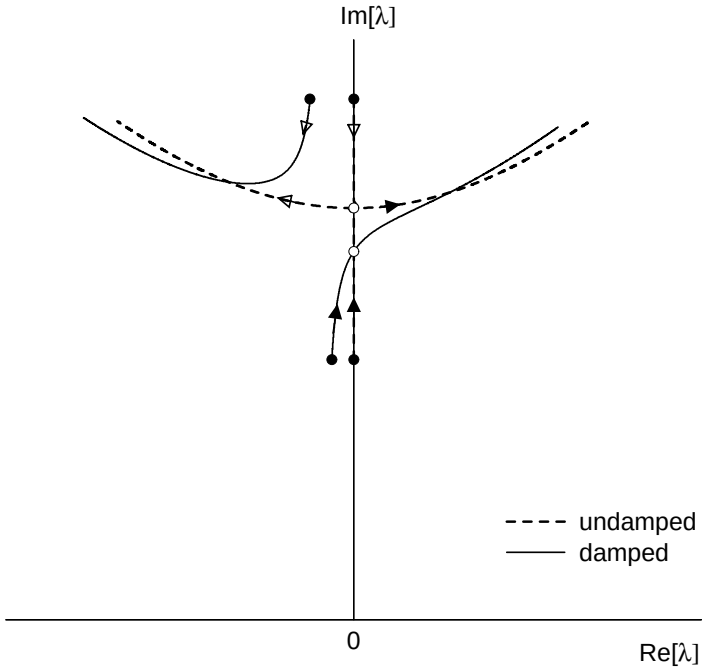

Figure 2: Complex plane representation of eigenvalue evolution as a function of control parameter α (adapted from Bolotin [49]). The dotted lines illustrate an example of the eigenvalues for a system of two coupled oscillators without damping, while the solid lines illustrate the same system with damping. Filled circles represent eigenvalues evaluated at $\alpha = 0$; unfilled circles represent Hopf bifurcations at $\alpha = \alpha_t$.

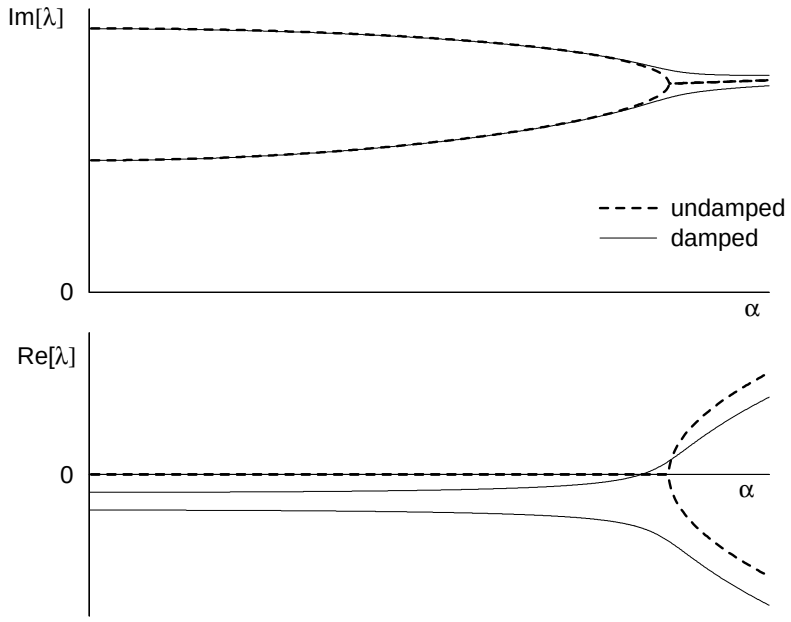

Figure 3: Imaginary and real parts of eigenvalues as a function of a control parameter, α, which is characteristic of the flow. This figure demonstrates coalescence of eigenfrequencies (imaginary parts of eigenvalues), in the undamped case, because of the flow coupling effect. The introduction of structural damping lowers the threshold value of α.

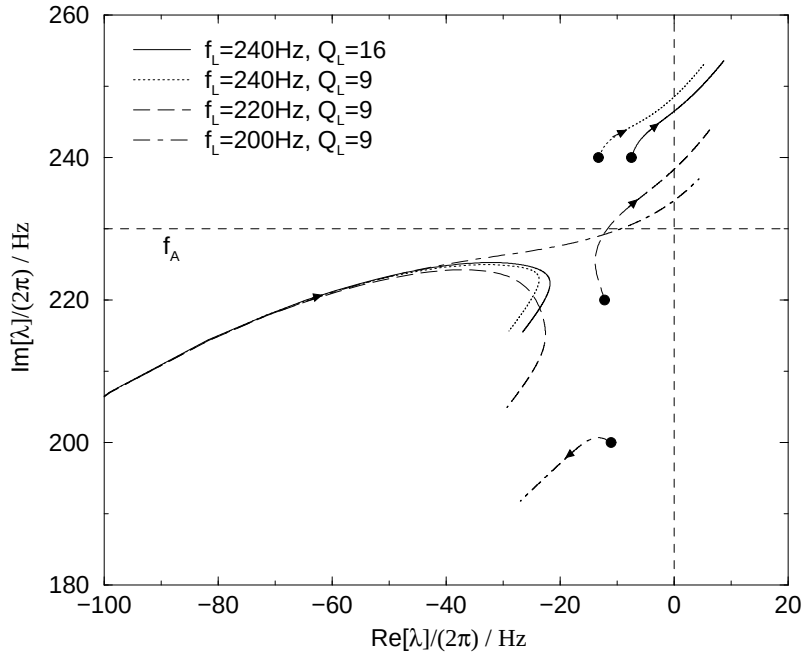

Figure 4: Complex plane representation of eigenvalue evolution as a function of $\overline{P_m}$ for four different sets of mechanical parameters. In each case $1/\mu_L = 0.09\,\mathrm{m^2 kg^{-1}}$, $f_A = 230\,\mathrm{Hz}$, $Q_A = 24$, and $Z_A = 20\,\mathrm{M}\,\Omega$. Here and elsewhere $1\,\Omega = 1\,kg\,m^{-4}\,s^{-1}$.

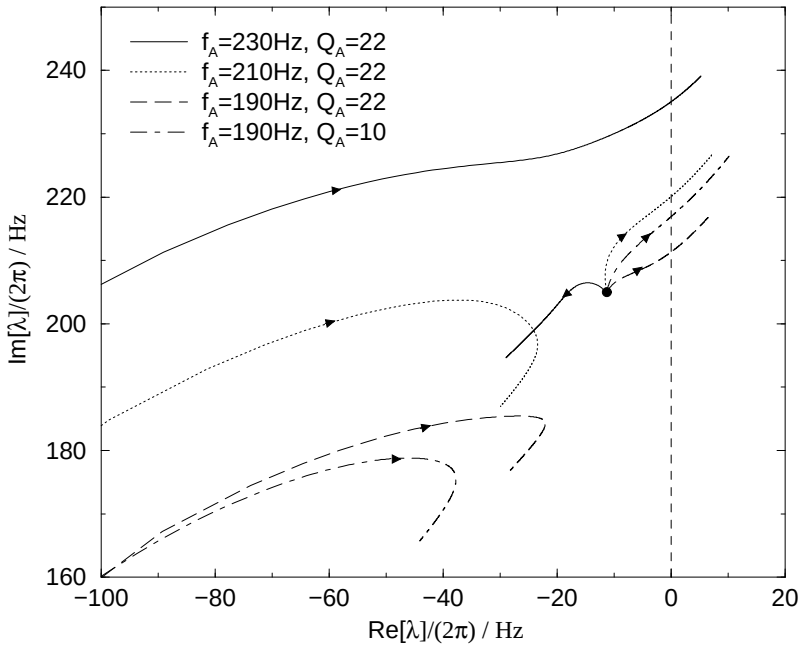

Figure 5: Complex plane representation of eigenvalue evolution as a function of $\overline{P_m}$ for four different sets of acoustical parameters. In each case $Z_A = 20\,\mathrm{M}\Omega$, $f_L = 205\,\mathrm{Hz}$, $Q_L = 9$, and $1/\mu_L = 0.09\,\mathrm{m}^2\mathrm{kg}^{-1}$.

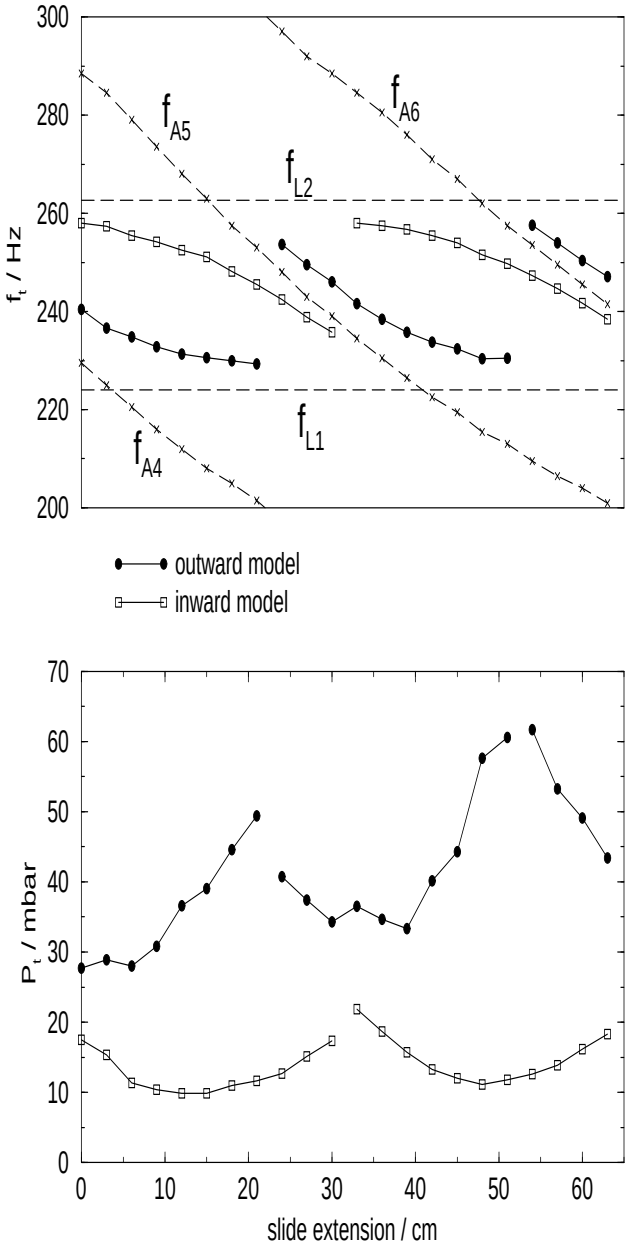

Figure 6: Trombone threshold values simulated using the inward striking model and the outward striking model. The embouchure was held constant as the slide extension was varied. Threshold frequencies are compared with resonance frequencies of the 4th, 5th and 6th acoustical modes of the trombone. Acoustical parameters (listed in table A of the Appendix) were extracted from input impedance measurements. Lip parameters used: $f_{L1} = 224\,\mathrm{Hz}$, $Q_{L1} = 9.0$, $1/\mu_{L1} = 0.09\,\mathrm{m^2kg^{-1}}$; $f_{L2} = 261\,\mathrm{Hz}$, $Q_{L2} = 14.5$, $1/\mu_{L2} = -0.11\,\mathrm{m^2kg^{-1}}$.

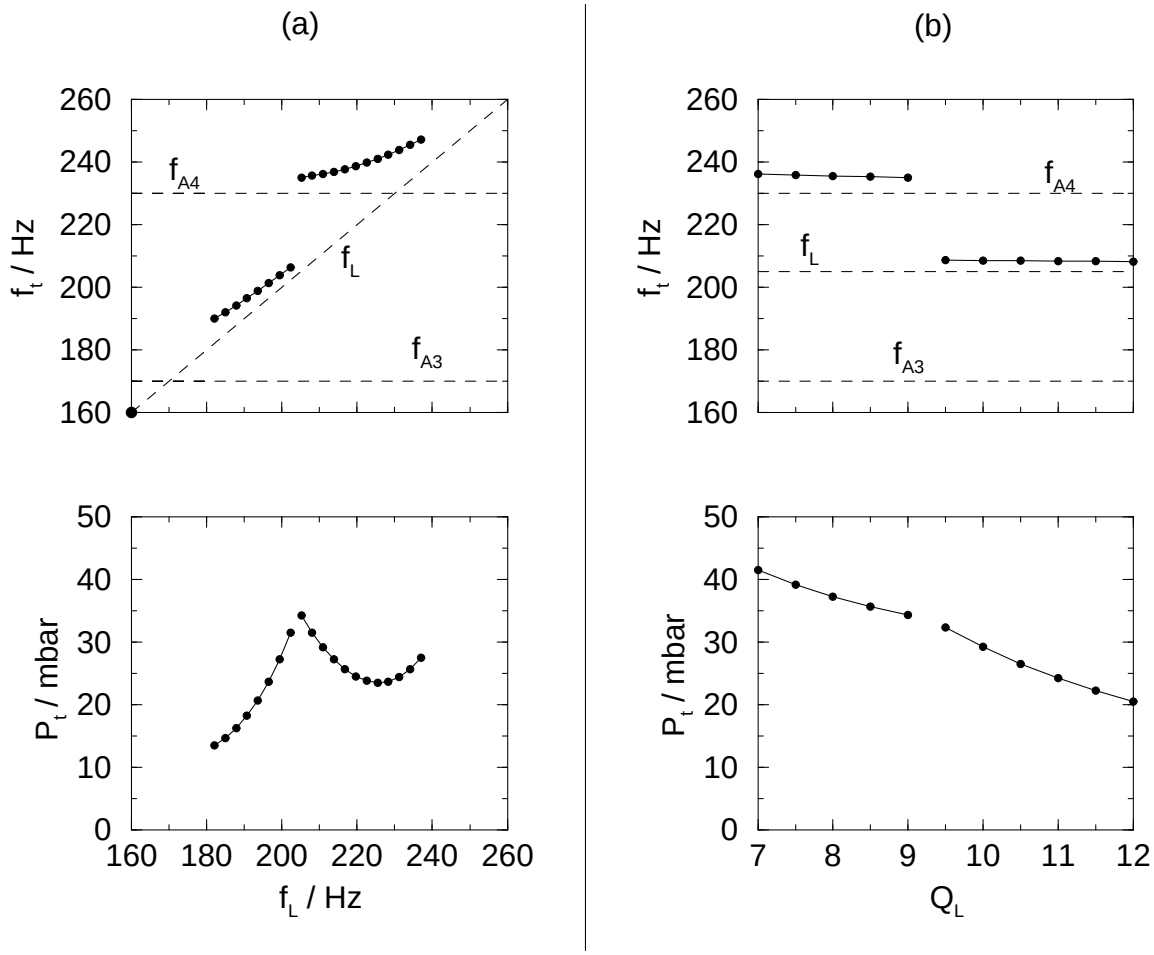

Figure 7: Trombone threshold values simulated using the outward striking model. The slide remained unextended while (a) the natural resonance frequency of the lip was increased and (b) lip quality factor was increased. Parameters used to obtain figures (a) and (b): $f_{A3} = 170\,\mathrm{Hz}$, $Q_{A3} = 18$, $Z_{A3} = 20\,\mathrm{M\Omega}$; $f_{A4} = 230\,\mathrm{Hz}$, $Q_{A4} = 24$, $Z_{A4} = 20\,\mathrm{M\Omega}$; $1/\mu_L = 0.09\,\mathrm{m^2 kg^{-1}}$. In figure (a) $Q_L = 9$; in figure (b) $f_L = 205\,\mathrm{Hz}$.

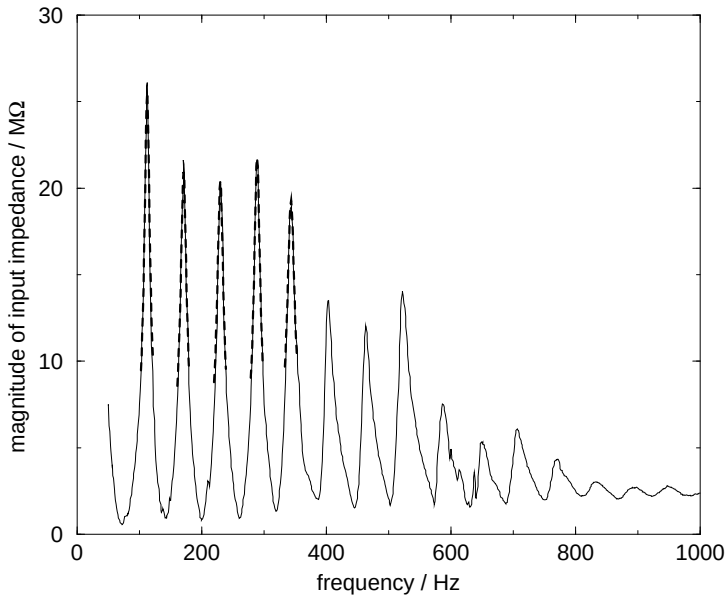

Figure 8: Measured input impedance magnitude of trombone with slide unextended (solid line) and least squares fit to modes 2 to 6 (dashed line).

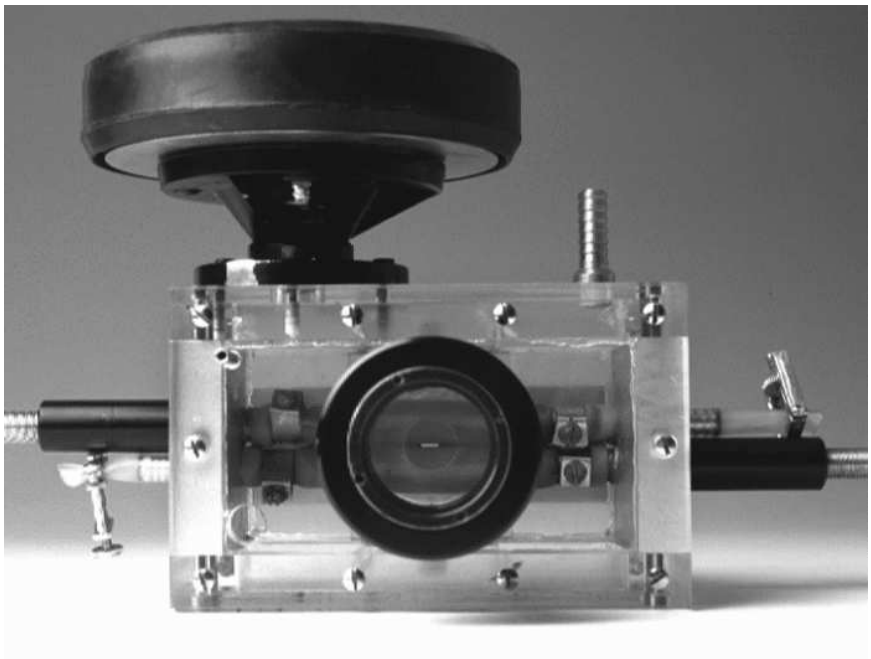

Figure 9: Photograph of artificial mouth, looking at the lips through the teeth.

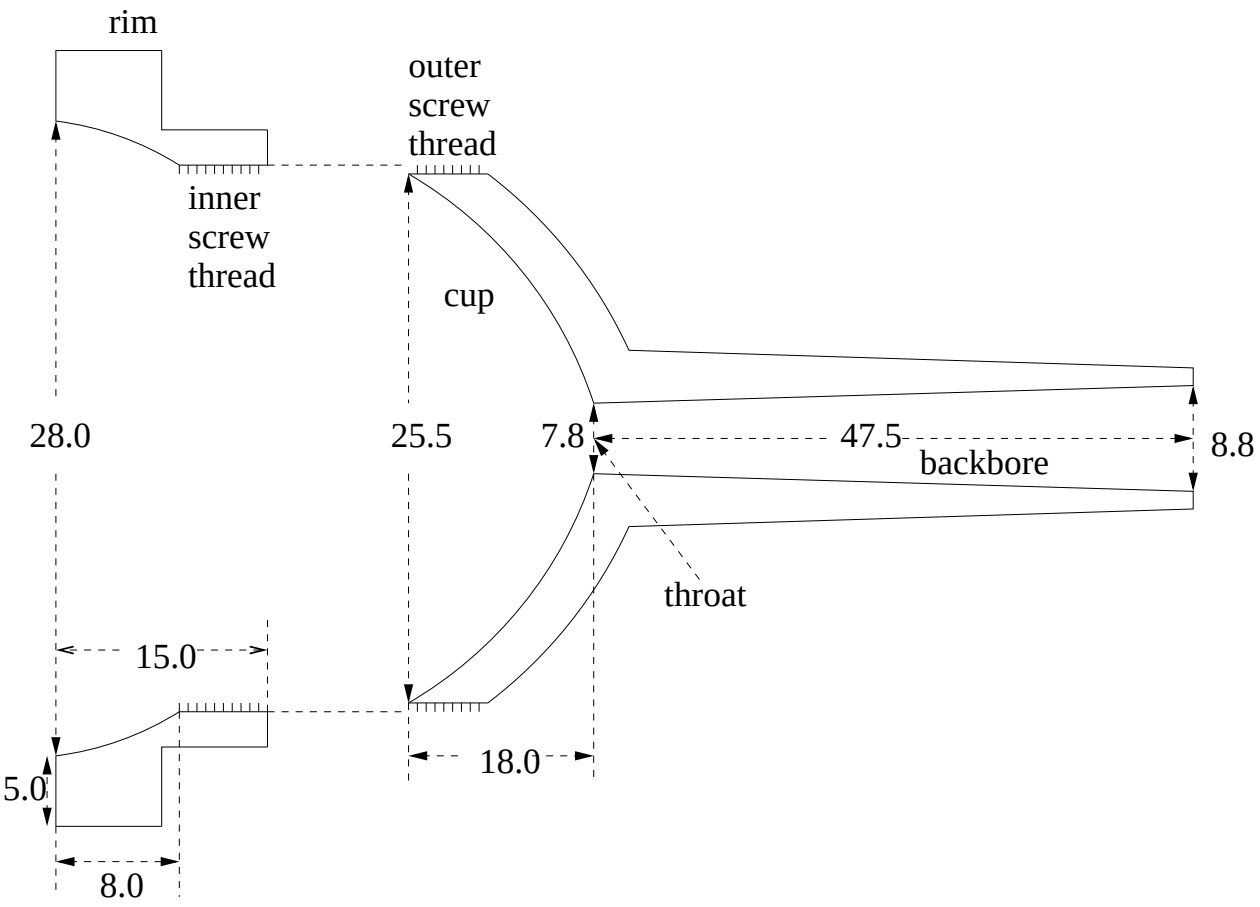

Figure 10: Cross-sectional view of two-piece mouthpiece showing the cup section remove from the rim. The numbers in the figure indicate dimensions in mm.

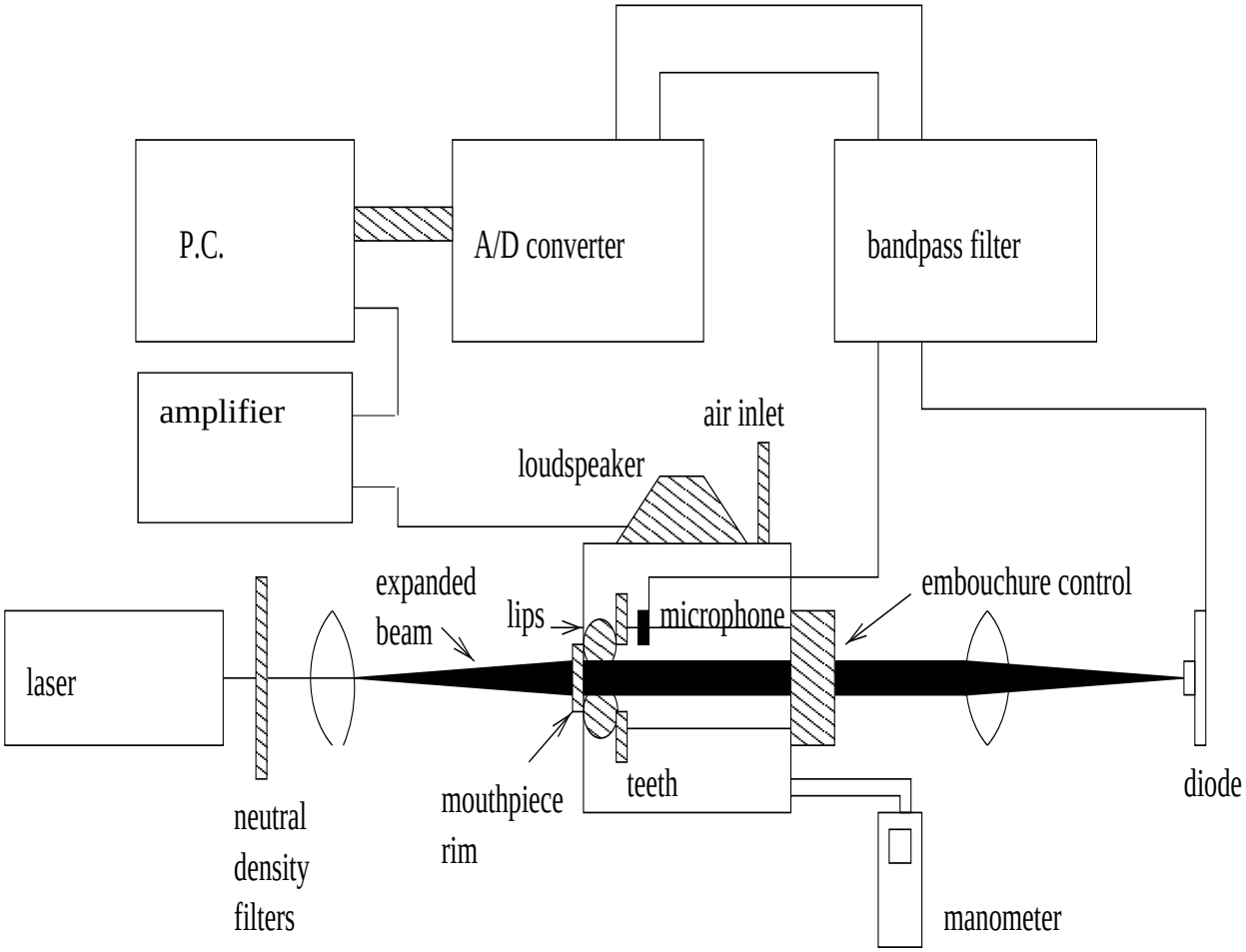

Figure 11: Apparatus for measuring mechanical response of artificial lip reed.

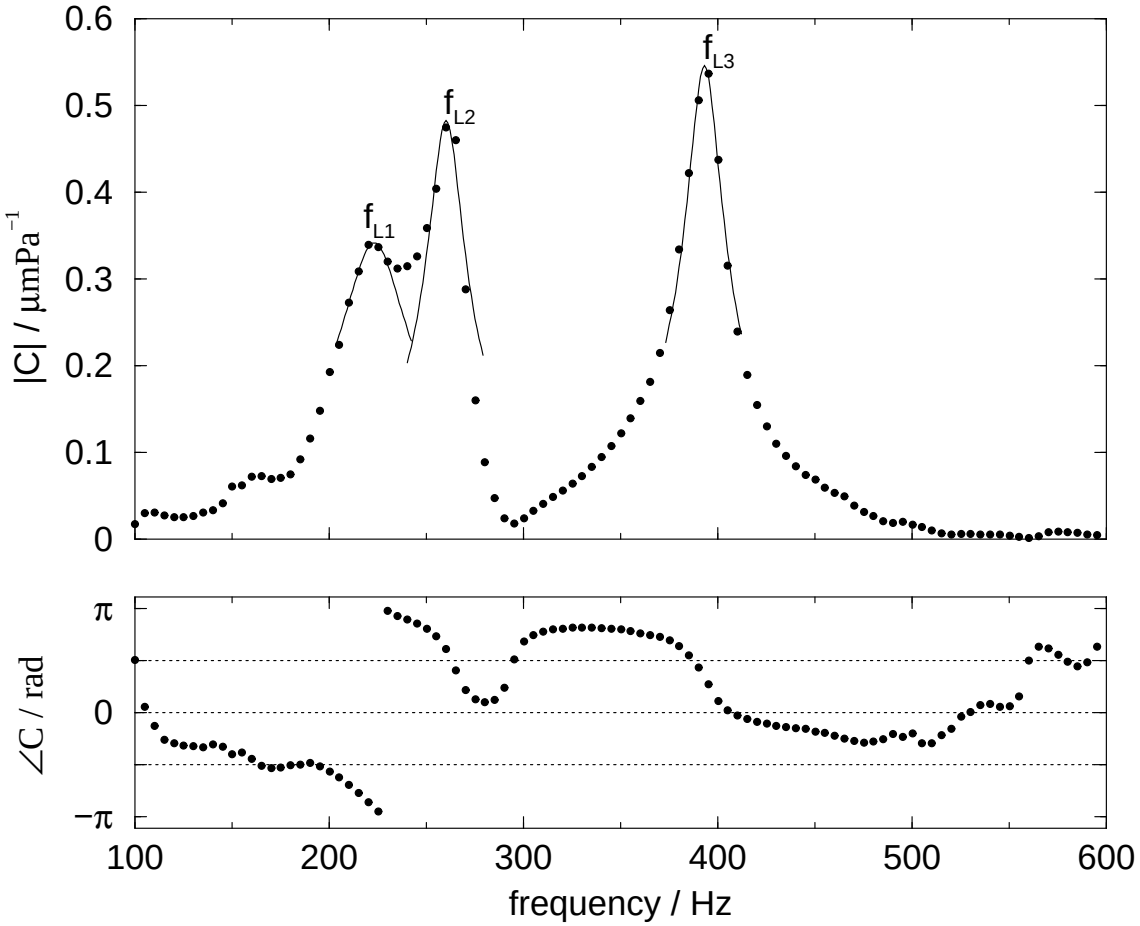

Figure 12: Measured mechanical response of artificial lip reed with tight embouchure (entire mouthpiece fitted). A static mouth pressure of 18.3 mbar was applied.

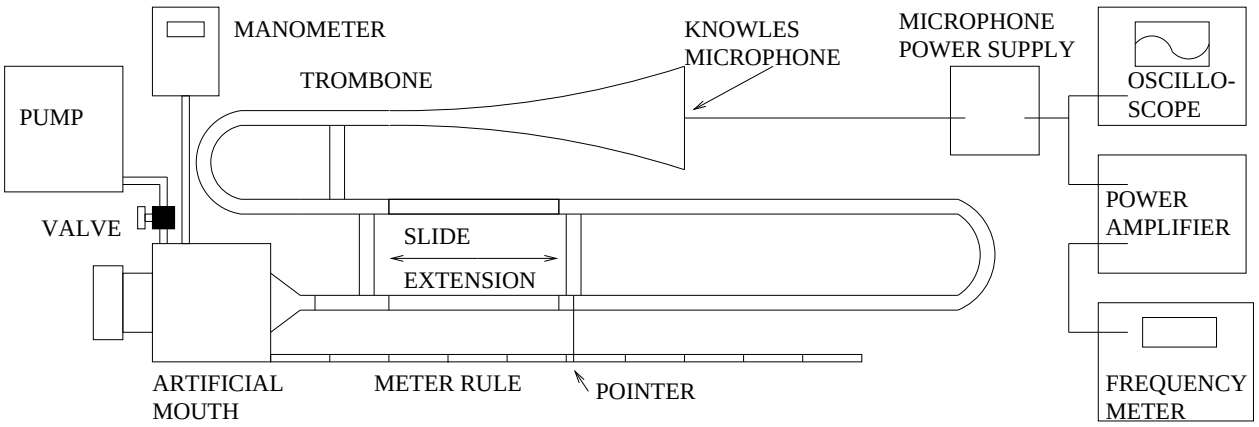

Figure 13: Apparatus for measuring threshold pressure and frequency.

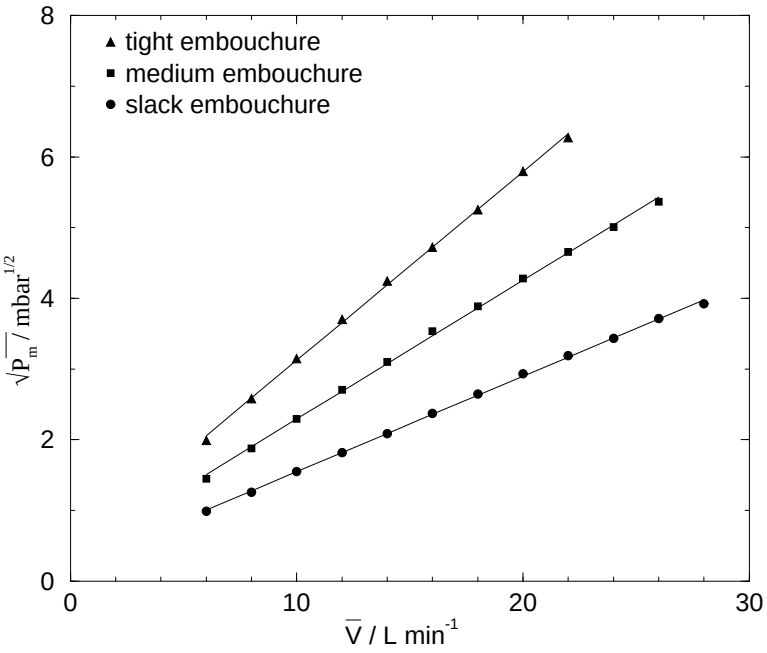

Figure 14: Measured variation of $\sqrt{\overline{P_m}}$ with $\overline{V}$ for 3 different embouchures.

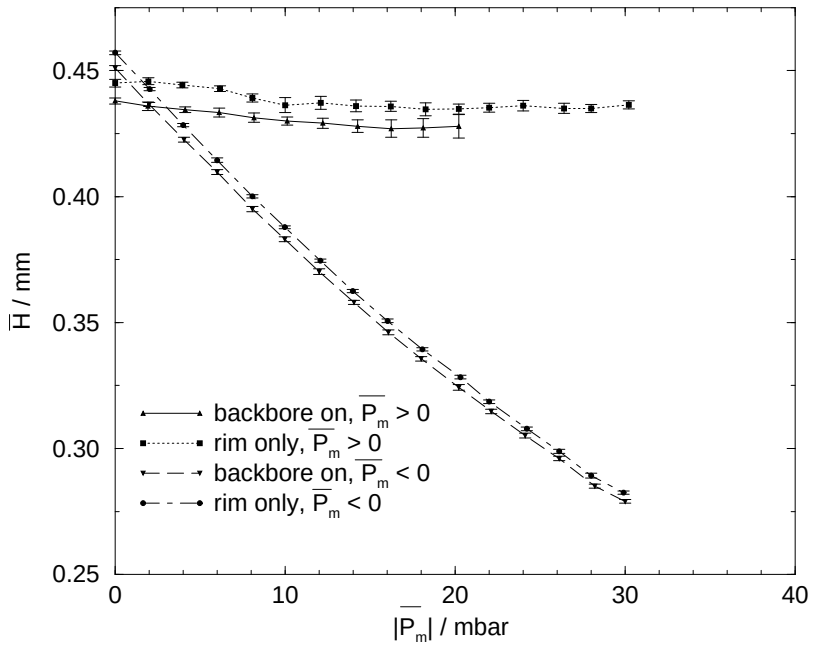

Figure 15: Measured variation of $\overline{H}$ with $\overline{P_m}$ for tightest embouchure. No periodic forcing of lips or self-excitation.

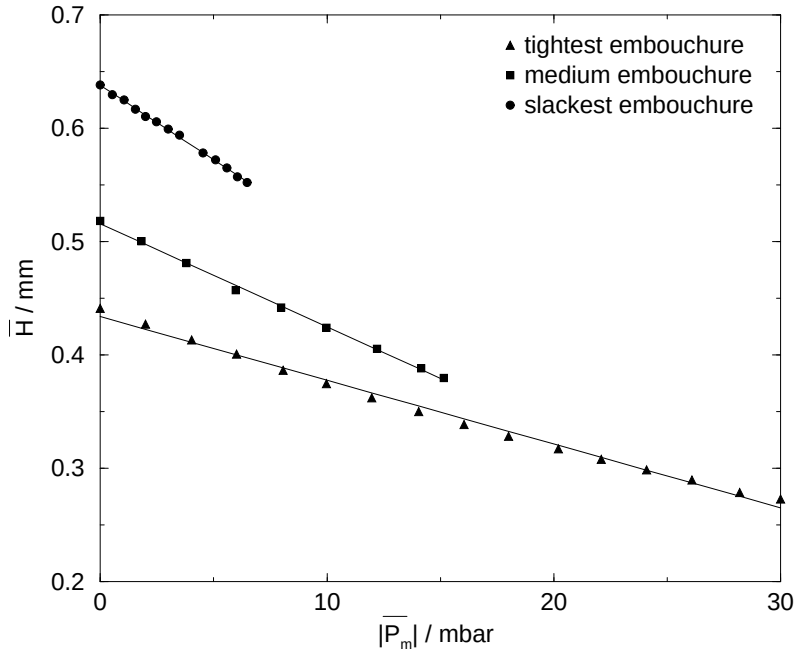

Figure 16: Measured variation of $\overline{H}$ with $\overline{P_m}$ for 3 different embouchures. In each case measurements were carried out with the cup removed and with $\overline{P_m} \leq 0$.

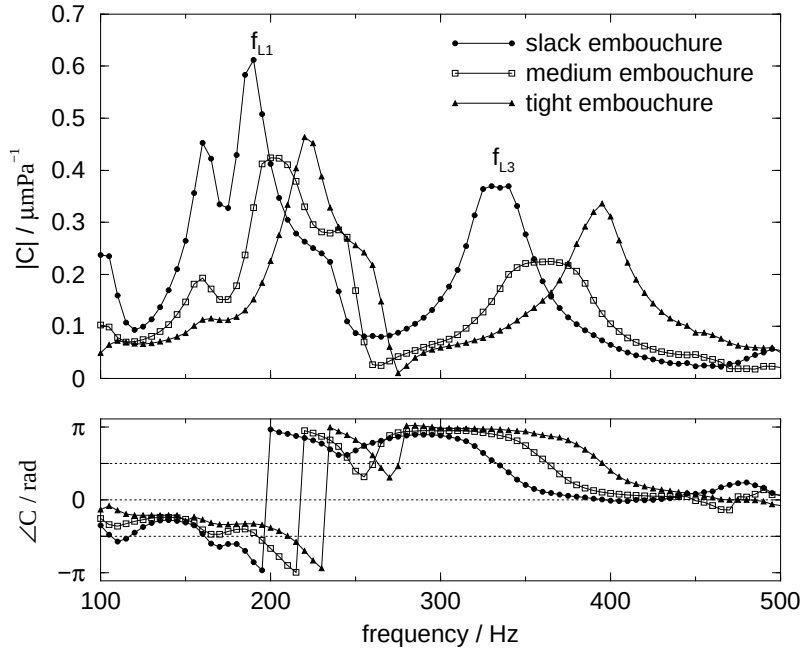

Figure 17: Mechanical response of the three embouchures with $\overline{P_m} = 0$ (mouthpiece cup removed).

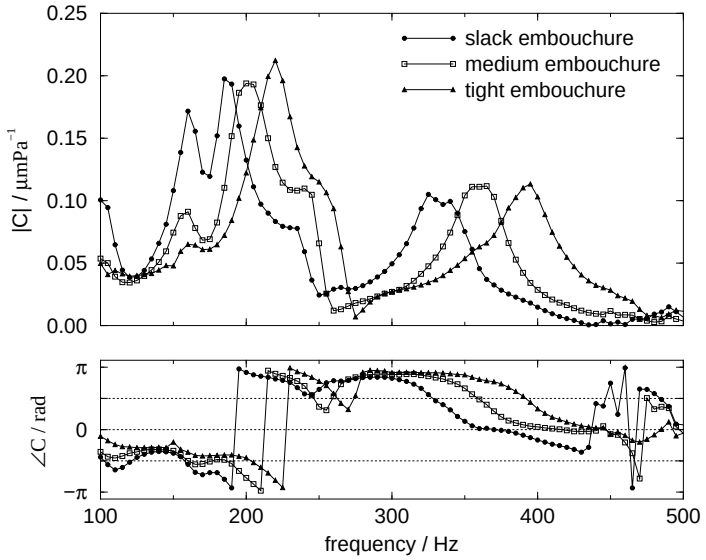

Figure 18: Mechanical response of the three embouchures with $\overline{P_m} = 0$ (entire mouthpiece fitted).

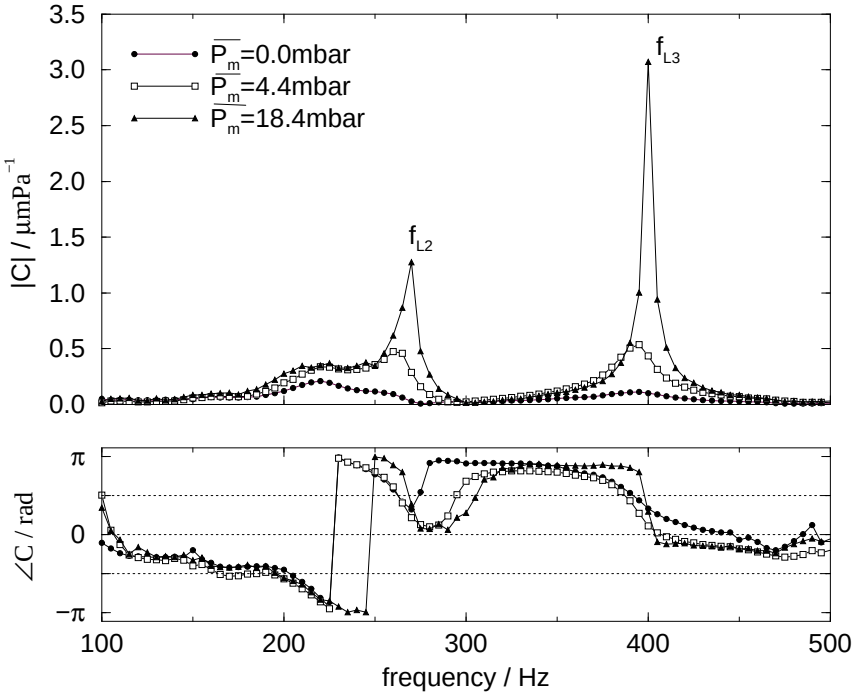

Figure 19: Mechanical response of tightest embouchure with different values of $\overline{P_m}$ (entire mouthpiece fitted).

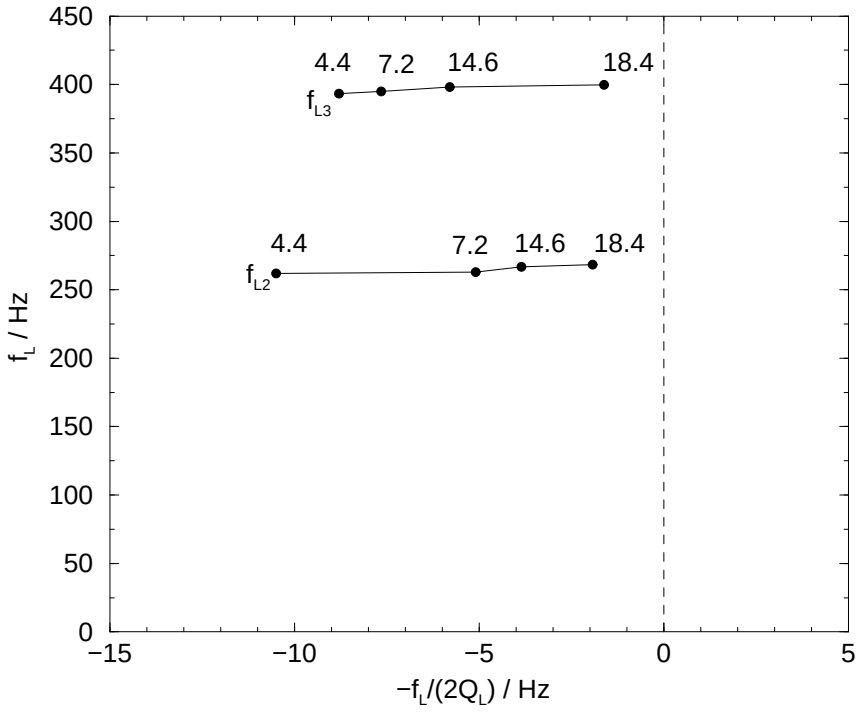

Figure 20: Complex plane representation of measured mechanical response of tightest embouchure (entire mouthpiece fitted). The numbers beside each point indicate $\overline{P_m}$, in mbar.

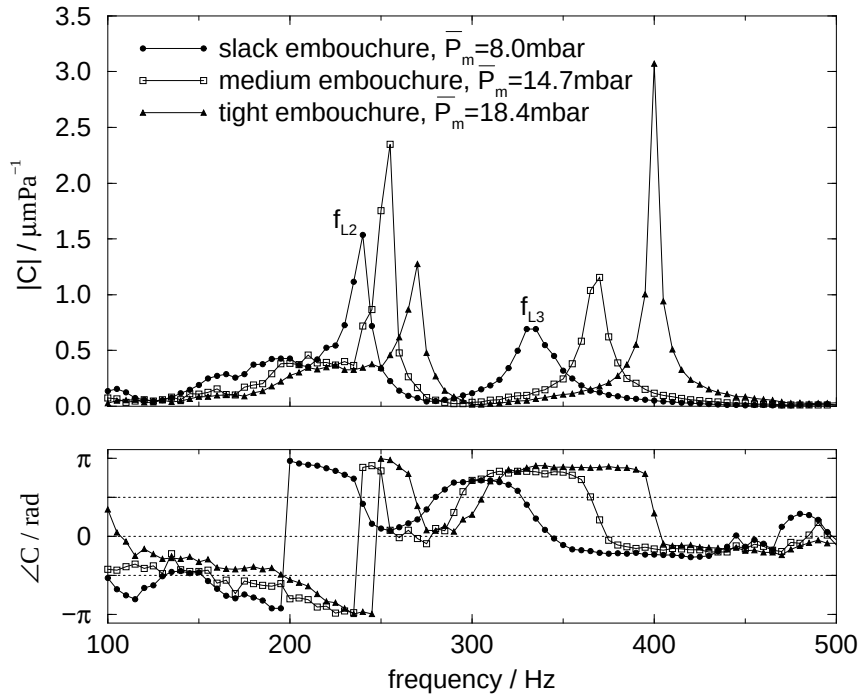

Figure 21: Mechanical response of the three embouchures with $\overline{P_m}$ slightly below oscillation threshold (entire mouthpiece fitted).

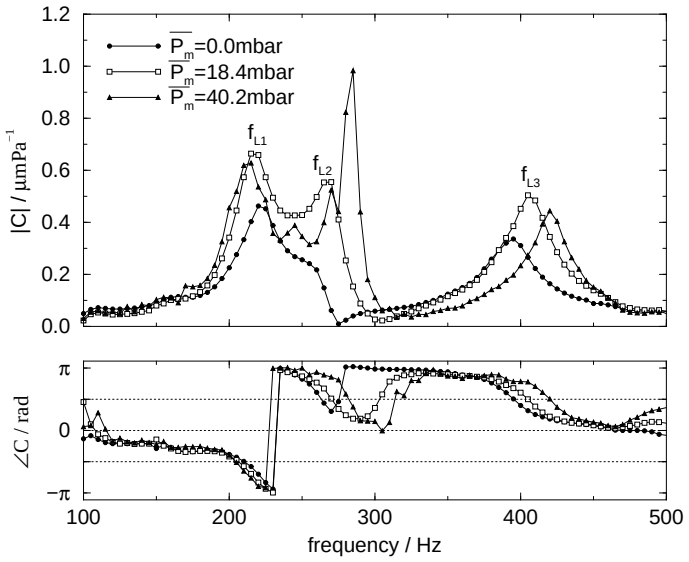

Figure 22: Mechanical response of the tightest embouchure with different values of $\overline{P_m}$ (mouthpiece cup removed).

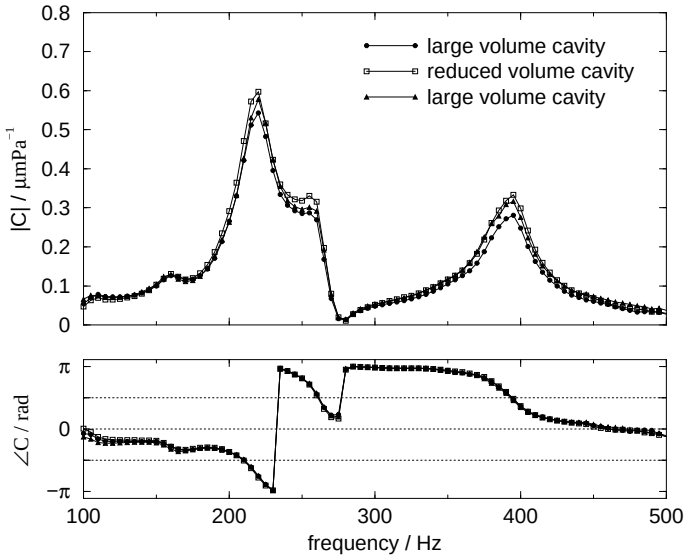

Figure 23: Mechanical response measurements with different mouth cavity volumes. Measurements carried out with cup removed and $\overline{P_m} = 0$.

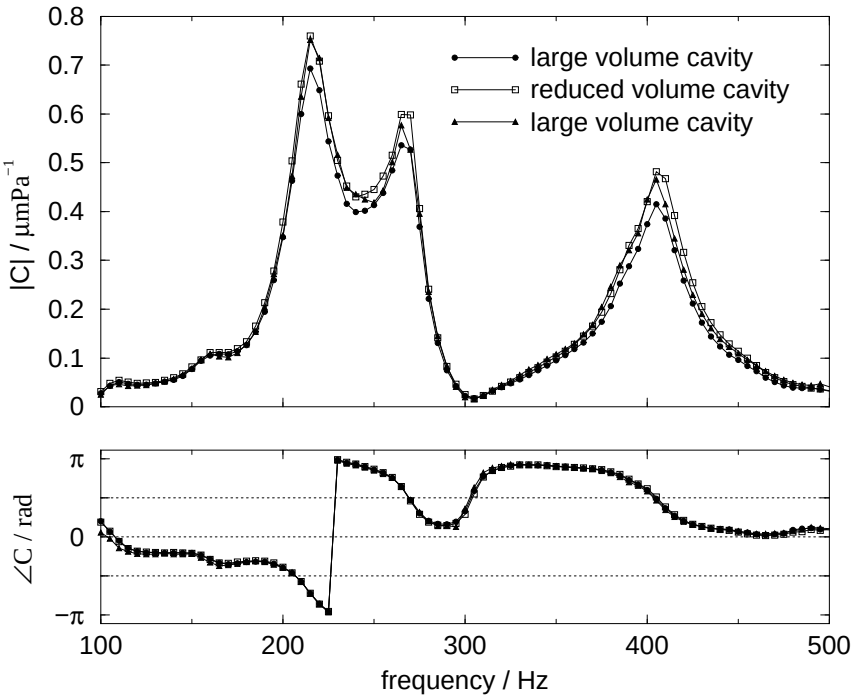

Figure 24: Mechanical response measurements with different mouth cavity volumes. Measurements carried out with cup removed and $\overline{P_m} = 18.4\,\mathrm{mbar}$.

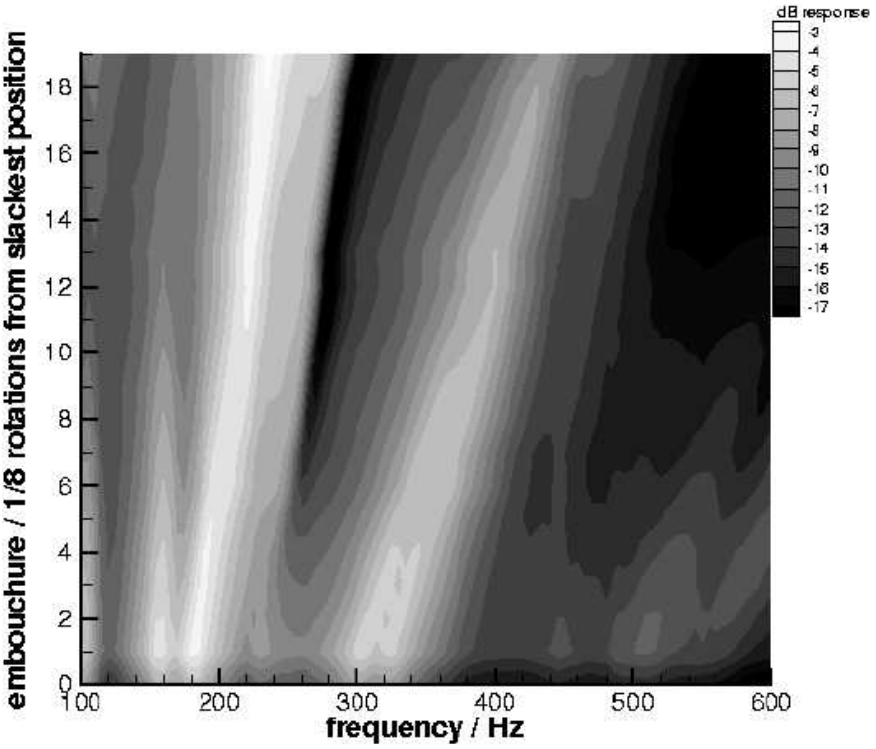

Figure 25: Contour map of mechanical response magnitude as a function of embouchure and frequency. Measurements performed with mouthpiece cup removed and $\overline{P_m} = 0$.

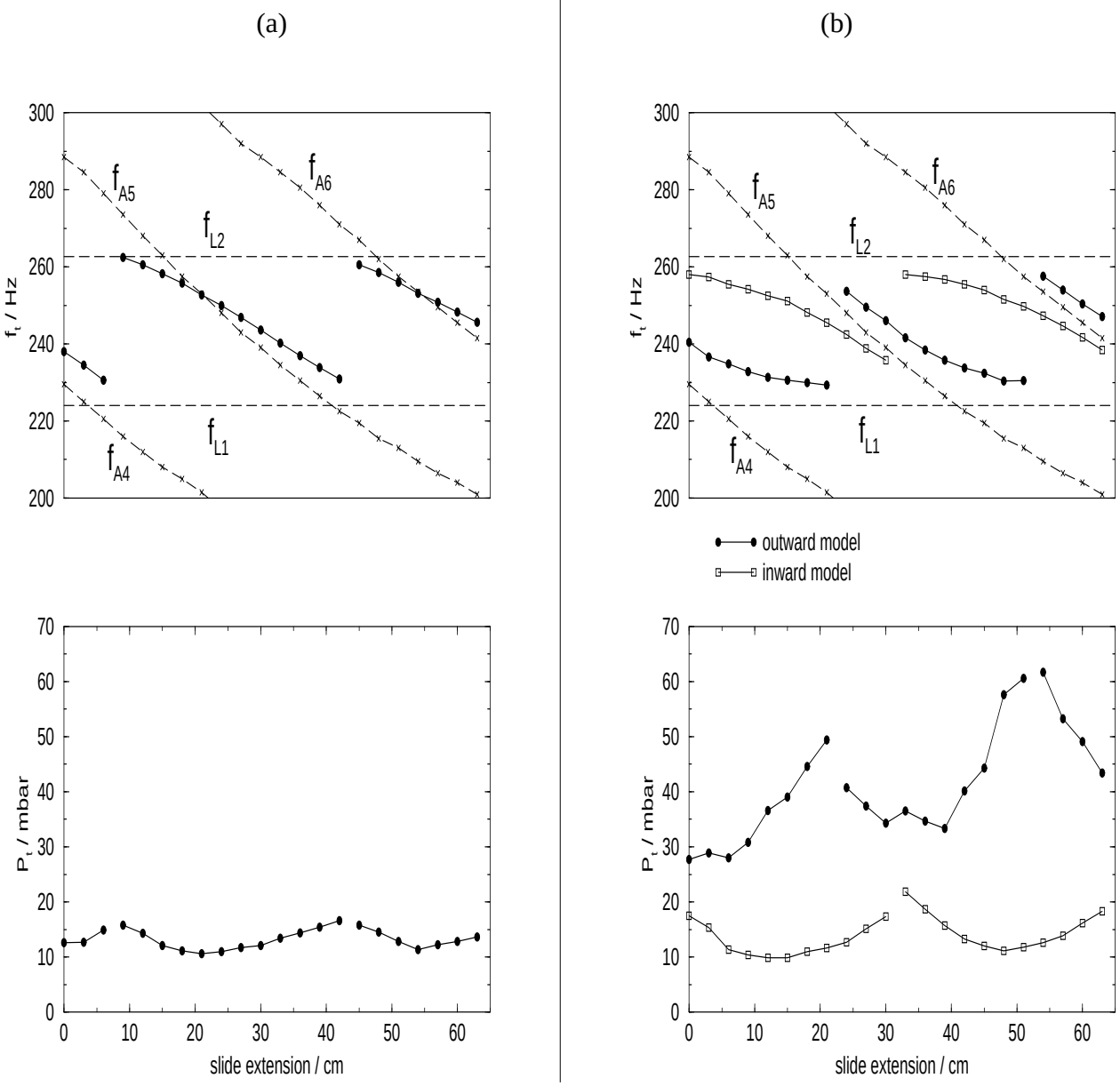

Figure 26: Variation of threshold valuves with slide position (fixed embouchure). (a) Measured threshold behaviour. (b) Threshold behaviour simulated using the inward and outward one mass models with lip parameters estimated from mechanical response measurements (see table B). Lip parameters used: $f_{L1} = 224\,\mathrm{Hz}$, $Q_{L1} = 9.0$, $1/\mu_{L1} = 0.09\,\mathrm{m^2kg^{-1}}$; $f_{L2} = 261\,\mathrm{Hz}$, $Q_{L2} = 14.5$, $1/\mu_{L2} = -0.11\,\mathrm{m^2kg^{-1}}$.

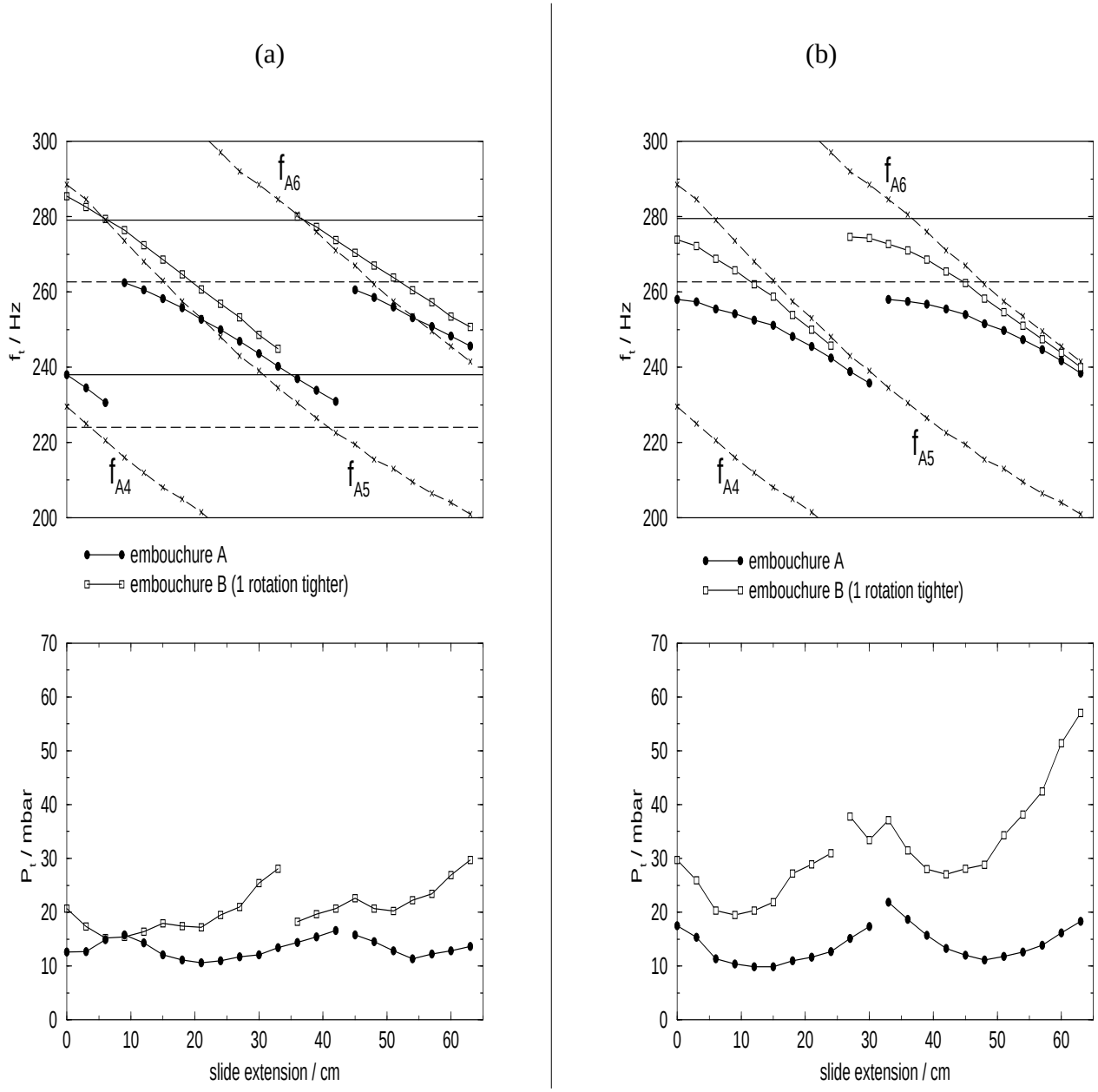

Figure 27: Variation of threshold values with slide position for two different embouchures. The horizontal lines indicate the lip resonance frequencies for embouchure A (dashed lines) and embouchure B (solid lines). (a) Measured threshold behaviour. (b) Threshold behaviour simulated using the inward one mass model. Embouchure A parameters: $f_{L2} = 261\,\mathrm{Hz}$, $Q_{L2} = 14.5$, $1/\mu_{L2} = -0.11\,\mathrm{m^2kg^{-1}}$. Embouchure B parameters: $f_{L2} = 279.5\,\mathrm{Hz}$, $Q_{L2} = 10.5$, $1/\mu_{L2} = -0.08\,\mathrm{m^2kg^{-1}}$.

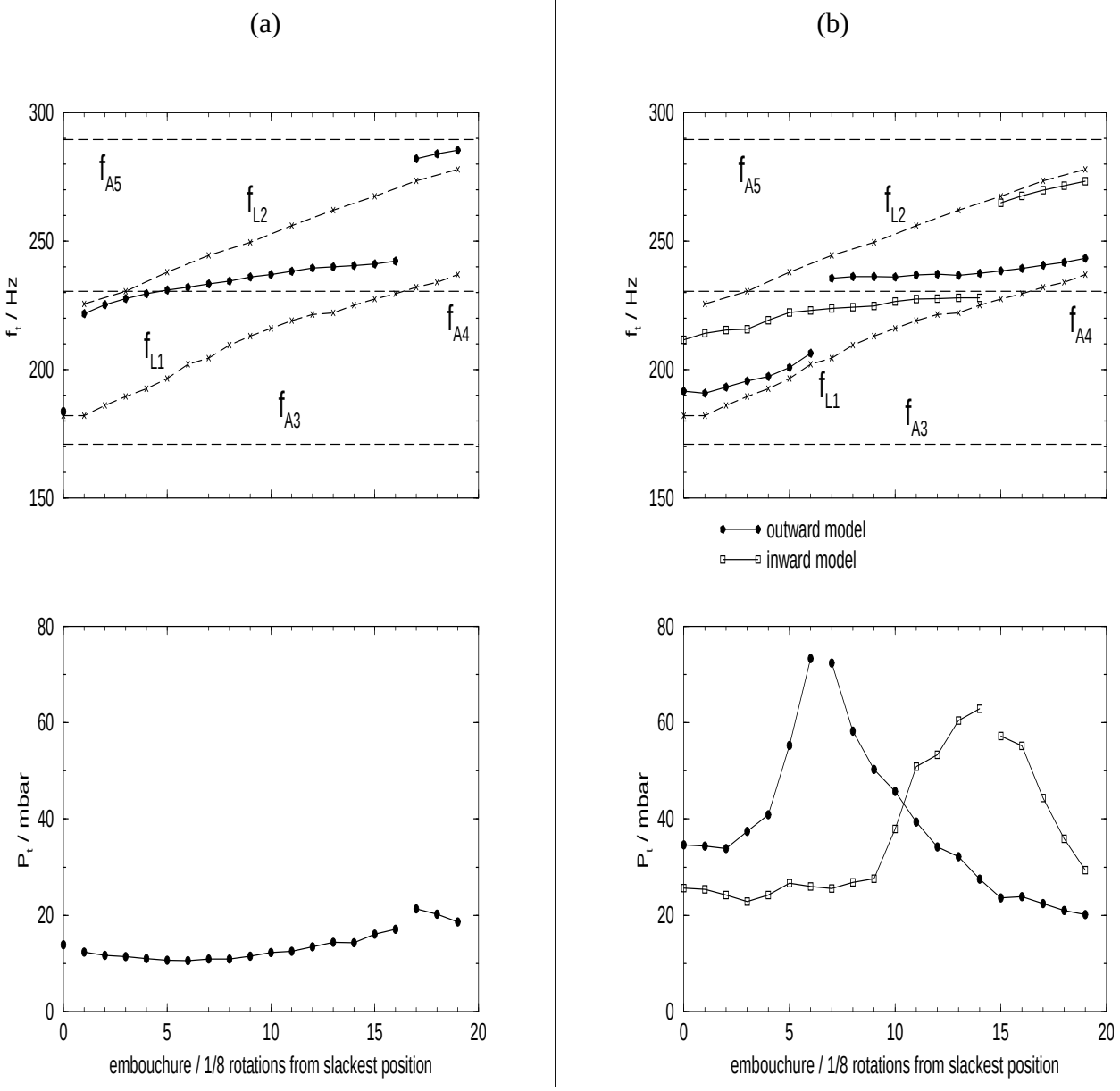

Figure 28: Variation of threshold values with embouchure, the trombone slide remains unextended. (a) Measured threshold behaviour. (b) Threshold behaviour simulated using the inward and outward one mass models with lip parameters estimated from mechanical response measurements (see table B of the appendix). Acoustical parameters: $f_{A3} = 170.5\,\mathrm{Hz}$, $Z_{A3} = 21\,\mathrm{M\Omega}$, $Q_{A3} = 19$; $f_{A4} = 229.5\,\mathrm{Hz}$, $Z_{A4} = 20\,\mathrm{M\Omega}$, $Q_{A4} = 24$; $f_{A5} = 288.5\,\mathrm{Hz}$, $Z_{A5} = 22\,\mathrm{M\Omega}$, $Q_{A5} = 31.5$.

Tables

	slack	medium	tight
b / mm	15	12	11
$\overline{H_0}$ / mm	0.63	0.53	0.44
f_{L1} / Hz	189	203.5	222
Q_{L1}	10.5	6	9
$1/\mu_{L1}$ / $\mathrm{m^2kg^{-1}}$	0.07	0.11	0.09
f_{L2} / Hz	234	resonance	259.5
Q_{L2}	11	not clearly	10.5
$1/\mu_{L2}$ / $\mathrm{m^2kg^{-1}}$	-0.13	resolved	-0.11
f_{L3} / Hz	338.5	362	394
Q_{L3}	8	4	13
$1/\mu_{L2}$ / $\mathrm{m^2kg^{-1}}$	-0.30	-0.26	-0.14

Table 1: Parameters for embouchures 'slack', 'medium' and 'tight' estimated from static and dynamic mechanical response measurements.

	present study	Elliot & Bowsher [2]	Saneyoshi et al [24]
b / mm	9 – 18	13	8.8 – 10.5
$\overline{H_0}$ / mm	0.25 – 0.70	0.30 – 0.45	0.07 – 0.17
f_{L1} / Hz	182 – 237	N.A.	N.A.
Q_{L1}	6 – 12	0.5	N.A.
$1/\mu_{L1}$ / $\mathrm{m^2kg^{-1}}$	0.04 – 0.11	0.3 – 0.6	N.A.
f_{L2} / Hz	225 – 278	N.A.	N.A.
Q_{L2}	8 – 16	0.5	5
$1/\mu_{L2}$ / $\mathrm{m^2kg^{-1}}$	-0.05 – -0.13	-0.5 – -0.7	-0.19 – -0.27

Table 2: Comparison of parameter ranges measured in present study with parameter ranges used in previous studies. Both of the previous studies [2] [24] considered a much larger range of lip resonance frequencies than in the present study, so f_{L1} and f_{L2} have been deemed not applicable (N.A.). Also, Saneyoshi et al [24] did not consider the outward striking reed case so f_{L1}, Q_{L1} and $1/\mu_{L1}$ are not applicable (N.A.).

present study	Elliot & Bowsher [2]	Saneyoshi et al [24]
b	l	b
$\overline{H_0}$	X_0	$\overline{d}$
$\frac{1}{\mu_{L1}}$	$\frac{A}{m}$	N.A.
$\frac{1}{\mu_{L2}}$	$-\frac{A_2}{m}$	$-\frac{A}{m'}$

Table 3: Relationship between parameters in present study and parameters used in previous studies [2] [24].

Appendix: Tables of measured acoustical and mechanical parameters

slide extension /cm	f_{A4} /Hz	Z_{A4} /MΩ	Q_{A4}	f_{A5} /Hz	Z_{A5} /MΩ	Q_{A5}	f_{A6} /Hz	Z_{A6} /MΩ	Q_{A6}
0	229.5	20	24.0	288.5	22	31.5	343.0	19	29.5
3	225.0	18	26.5	284.5	20	28.5	335.0	17	23.5
6	220.5	20	26.5	279.0	21	25.0	329.0	20	29.0
9	216.0	20	26.5	273.5	21	25.0	322.5	19	26.0
12	212.0	19	26.0	268.0	21	25.0	317.0	20	33.0
15	208.0	20	25.0	263.0	21	28.0	311.0	20	33.5
18	205.0	19	23.5	257.5	19	24.0	306.5	18	33.5
21	201.5	20	24.0	253.0	20	24.5	302.0	19	26.5
24	197.0	21	25.0	248.0	21	27.0	297.0	20	26.5
27	194.0	20	25.0	243.0	19	25.5	292.0	20	28.5
30	190.5	19	23.5	239.0	18	26.5	288.5	21	33.5
33	187.5	13	24.0	234.5	14	27.5	284.5	15	27.5
36	184.0	14	22.5	230.5	14	29.5	280.5	15	28.0
39	180.5	14	21.5	226.5	15	32.0	276.0	15	28.5
42	177.5	15	25.5	222.5	13	28.0	271.0	15	28.5
45	174.5	15	22.0	219.5	13	28.0	267.0	15	27.5
48	171.0	15	22.0	215.5	13	31.0	262.0	16	26.5
51	168.5	15	22.5	213.0	12	24.5	257.5	15	28.0
54	165.5	16	23.0	209.5	13	27.5	253.5	15	27.5
57	163.0	15	20.5	206.5	12	27.5	249.5	15	28.0
60	160.5	15	23.0	204.0	12	28.5	245.5	14	27.5
63	158.0	15	22.0	201.0	12	27.5	241.5	14	27.0

Table A: Acoustical parameters of modes 4, 5 and 6, extracted from input impedance measurements of trombone. Note that $1\,\Omega = 1\,kg\,m^{-4}\,s^{-1}$. These parameters were used to produce figures 6, 26b and 27b.

embouchure	$\overline{H_0}$ /mm	b /mm	f_{L1} /Hz	Q_{L1}	$1/\mu_{L1}$ /m^2kg^{-1}	f_{L2} /Hz	Q_{L2}	$1/\mu_{L2}$ /m^2kg^{-1}
0	**0.70**	**18**	182.0	9.5	0.044	**223.0**	**9.2**	**−0.065**
1	**0.68**	**17**	182.0	10.0	0.041	225.5	10.5	−0.059
2	**0.65**	**16**	186.0	10.5	0.042	**228.0**	**9.8**	**−0.066**
3	0.63	15	189.5	10.5	0.042	230.5	8.0	−0.084
4	**0.61**	**14**	192.5	11.5	0.039	**234.2**	**10.2**	**−0.069**
5	**0.58**	**13**	196.5	10.0	0.044	238.0	12.5	−0.058
6	**0.56**	**13**	202.0	8.5	0.053	**241.2**	**11.8**	**−0.065**
7	0.53	12	204.5	7.0	0.063	244.5	11.0	−0.073
8	**0.51**	**12**	209.5	7.5	0.064	**247.0**	**10.8**	**−0.073**
9	**0.48**	**12**	213.0	8.5	0.059	249.5	10.5	−0.074
10	**0.46**	**11**	216.0	9.5	0.056	**252.8**	**13.2**	**−0.059**
11	0.44	11	219.0	9.5	0.059	256.0	16.0	−0.048
12	**0.41**	**11**	221.5	10.5	0.056	**259.0**	**15.8**	**−0.049**
13	**0.39**	**10**	222.0	11.0	0.057	262.0	15.5	−0.050
14	**0.37**	**10**	225.0	12.0	0.056	**264.8**	**14.8**	**−0.052**
15	**0.34**	**10**	227.5	12.0	0.059	267.5	14.0	−0.053
16	**0.32**	**9**	229.5	11.5	0.064	**270.5**	**13.0**	**−0.059**
17	**0.30**	**9**	232.0	11.5	0.067	273.5	12.0	−0.067
18	**0.27**	**9**	234.0	11.5	0.070	**275.8**	**12.2**	**−0.068**
19	**0.25**	**9**	237.0	12.0	0.072	278.0	12.5	−0.069

Table B: Lip parameters extracted from mechanical response measurements. Numbers in bold font indicate parameters which were estimated from extrapolating or interpolating neighbouring measured parameter values (standard font). The lip parameters in this table were used to produce figure 28b.